Physica D 495 (2026) 135289

Contents lists available at ScienceDirect

Physica D

journal homepage: www.elsevier.com/locate/physd

The early stage of the motion along the gradient of a concentrated vortex structure

Franco Flandoli [a], Matteo Palmieri [b], Milo Viviani [a,*]

[a] Scuola Normale Superiore, Pisa, Italy
[b] Max Planck Institute for Mathematics in the Sciences, Leipzig, Germany

ARTICLE INFO

Communicated by Dr Ye Zhou

Keywords:
Zonal flows
Numerical simulations of 2D turbulence
Vortex-wave equations
Point vortex dynamics

ABSTRACT

We give a rigorous mathematical result, supported by numerical simulations, of the aggregation of a concentrated vortex blob with an underlying non-constant vorticity field: the blob moves in the direction of the gradient of the field. It is a unique example of a Lagrangian explanation of aggregation of vortex structures of the same sign in 2D inviscid fluids. The result is also extended to almost vertical vortex filaments in a (possibly thin) three-dimensional domain.

1. Introduction

Vortex structures emerge from many instabilities mechanisms of fluid and plasma dynamics, like Rayleigh-Taylor, Richtmyer–Meshkov, and Kelvin–Helmholtz instabilities [1–3]. In the case of 2D (or nearly two-dimensional) fluids, their interaction and in particular their merging properties play a fundamental role in many processes, like in the turbulent inverse cascade [4], in the emergence and dynamics of large scale structures in the atmosphere of certain planets [5,6] and in the poloidal section of confined fusion plasma [7,8]. Here and below we shall generically name it vorticity, meaning true vorticity for classical fluids, but potential vorticity for geophysical fluids, [9] and a particle density or the electrostatic potential - depending on the approximate model - for a plasma [10,11].

With a large degree of simplification, we may divide the mutual interaction of vortex structures and their interaction with background fields into two main classes.

a) The first class contains the interaction of vortex structures approximately of the same size (with small variants of different size but with the same order of magnitude [12]). The present paper is not devoted to this case, but we mention it for comparison and side remarks. When the two vortex structures have the same sign and are sufficiently close to each other, they merge into a larger structure (hence the energy previously incorporated in the smaller ones moves to the large final one, as the inverse energy cascade predicts) and produce very small scale structures like filaments (hence part of the vorticity, previously incorporated in the two initial structures, will be found in the very thin filaments, in agreement with the direct enstrophy cascade [13]). This process has been widely investigated, in particular for the potential vorticity field in geostrophic dynamics and turbulence [14–16], and has been experimentally observed and investigated in the case of the oval BA (Red Spot Jr.) of Jupiter [17–20]; but it has been also studied for simplified plasma models, see for instance [21] and references therein.

b) The second class contains the case of interaction of vortex structures of very different sizes, so that one looks almost pointwise compared to the other. Similarly, it contains the case of the interaction between an almost pointwise structure and a background shear flow. It is called the vortex-wave problem in the limit of a pointwise vortex [22]; the small vortex structures are also often called clumps and holes [23]. In this category, we may also insert the beta-drift problem, namely the motion of a concentrated vortex structure in the presence of Coriolis force, relevant for instance to the motion of cyclones in the atmosphere [24–26]. The interaction of very concentrated vorticity structures with much larger vortex structures or a vorticity background may be important to understand the properties (e.g. energy maintenance, growth and shaping) of large scale structures (like zonal flows or streamers) in planets and plasma [6,7,27].

Case (a) is documented by several numerical studies, but it is less clear from the theoretical point of view based on the equations of motion, with some information extracted by statistical mechanics arguments related, for instance , to the concept of entropy [12,28], or Onsager theory [29]. As already said above, we have mentioned case (a) for comparison, but it will not be the main object of this work.

Case (b) is more amenable to an analytical theory, because of the presence of a small parameter (the ratio between the scales of the two structures) and because in some regimes or small time one may assume

* Corresponding author.
E-mail addresses: franco.flandoli@sns.it (F. Flandoli), matteo.palmieri@mis.mpg.de (M. Palmieri), milo.viviani@sns.it (M. Viviani).

https://doi.org/10.1016/j.physd.2026.135289
Received 28 May 2025; Received in revised form 27 May 2026; Accepted 30 May 2026
Available online 4 June 2026

a moderate modification of the background. We focus here on this case. More precisely, we focus on a specific property of the interaction between a concentrated structure and a background: the *motion of the structure along the gradient of the background vorticity*. Beyond being of interest in itself, this particular property is in a loose sense a property of *aggregation* of vorticity structures having the same sign, thus with some analogy with the coalescence of similar size vortices mentioned in point (a) above. Moreover, there is some loose analogy also in some detail of the process, like the formation of a the strong shear layer between the structures during the merging process (a) [15,21] or the encapsulation process (b) [30,31].

We do not discuss in detail the rich literature focusing on other questions for (b) different from the question of the motion along the gradient. Among others, let us only mention the analysis of the oscillations of the concentrated vortex when it is close to the boundary of a large one and could lead to coalescence of the two [31] (containing an interesting hamiltonian analysis of the model); or the growth of holes and their dynamics [23] which contains many ideas and methods used later on by other authors.

We specifically recall, on the contrary, the experimental and numerical investigation of the motion along the gradient performed by Amoretti et al. [30] which highlights the complexity of the interaction layers between concentrated vortex and the interior of the large one. And the deep analytical analysis of the motion along the gradient by Schecter and Dubin [32], who found quantitative formulae for the motion, with good numerical fit in some case, and explain well also the heuristics behind the methodology, based on the idea of a strong local mixing of the background near the concentrated vortex, which produces a motion of the vortex by conservation of momentum.

In spite of the previously mentioned progress, which provided sure evidence that a motion along the gradient exists and understood some of its features, a rigorous mathematical proof, without approximations, does not exist. For instance, the analytical computation of [32] is based on a sequence of two approximations: first a formula for the approximate deformation of the background field produced by the very strong action of the concentrated vortex structure; then an approximate formula for the displacement caused by the deformed field on the structure. These approximations are very realistic and implementing them in sequence instead of in parallel (in spite of the fact that the two actions happen simultaneously) looks an acceptable approximation in view of the difficulty of the problem. However, we see two criticalities. The first one is the lack of rigorous proof. Maybe more important, the great difficulty to extend the argument to problems which are similar but more complex, where other approximations hold simultaneously (each of them should then be under precise control for comparison, and it is not the case until now). We have in mind in particular the *quasi-two-dimensional case*, of paramount importance see [33] and references therein. If the same approximation arguments of previous works are applied to quasi-2D structures, the link between the mathematical approximations, their 3D effects (potentially very strong) and the small parameters characterizing the quasi-2D set-up should be very clear.

Our primary aim in this paper is adding some information on the *initial stage* of the motion along the gradient. The initial stage is cleaner, since the background flow at time zero is assumed to be a shear flow. Later stages may be very complex, namely the background may suffer a strong modification. In certain experiments and real world problems the shear-flow structure of the background could be reinforced by some mechanism, the shear flow structure may be restored to some degree by other forces acting on the fluid (for instance a pressure difference maintained between two positions), and these factors could contribute to prolong the time where we observe a clean motion along the gradient. But in the numerical simulations of the basic model equations (the Euler equations without forces), the clump (or hole) typically has a strong influence on the background which alters too much its structure and makes quite unpredictable and complex the dynamics after short time; also the concentrated vortex structure undergoes transformations after short time [34]. Therefore we put ourselves in the idealized situation of a clump in a strict shear flow at time zero, and aim to understand the first dynamical phase, before it reaches an uncontrolled complexity. With this restriction to the first phase of the dynamics, our aim is to develop a completely rigorous analysis, based on the full nonlinear equations of motion, free of any assumption and approximation.

Among the advantages of an approach free from uncontrolled approximations, there is potentiality to be extended to more complex cases. Here we shall investigate a quasi-two-dimensional framework, namely a vortex filament in a 3D shear flow, under assumptions of small deviation from a 2D case. The equations for vortex filaments have a long story, are notoriously difficult and present potential singularities. The question investigated here, of the motion along the gradient of a background shear flow, is new but other aspects of the motion of filaments, like well posedness and singularities, has been studied for long time, see for instance [35–47] and other references in the technical sections below.

Concerning mathematically rigorous approaches to vortex dynamics, but for questions different from the one treated here, we are indebt to important contributions to non-pointwise vortex structures [41,48,49] and to the dynamics of point vortices and its statistical mechanics properties, among others [49–56]. These results are not directly related to our work but they are generically in the background of our investigation. Other more directly related references will be quoted below in the technical sections.

The numerical simulations performed in the literature on these problems are various, with some preference for the particle-in-cell method [30]. We shall explore the performances of a variant of the Zeitlin model, on the rotating 2D sphere, that we call the vortex-wave Zeitlin model aiming to confirm the theoretical predictions.

In our problem the small intense vortex is not generated by the shear flow instability; the shear flow is still unperturbed at time $t = 0$, when the merging process starts. Clearly, the intrusion of the intense vortex in the shear flow will produce a strong perturbation of the latter, but we do not aim to give rigorous results on the evolution of the background perturbation, only on the initial-stage motion of the concentrated vortex in the direction of the initial gradient of the background vorticity.

Vortices in shear flow have also been considered from another viewpoint, see [57]. In that work, the authors found stable vortices stretched by the flow. But the basic assumption in that case is that the shear is constant, namely the vorticity is constant. Our result of motion along the vorticity gradient requires a non-zero vorticity gradient.

2. Local dynamics of the blob-wave system

In this section, for the sake of clarity of the calculations, we take as reference domain the flat torus $\mathbb{T}^2$. The Euler equation is the following nonlinear transport equation for the vorticity $\omega^t : \mathbb{T}^2 \to \mathbb{R}$ of fluid, advected by the velocity field $\mathbf{u}^t = (u_1^t, u_2^t) : \mathbb{T}^2 \to \mathbb{R}$ it generates

$$\partial_t \omega + \mathbf{u} \cdot \nabla \omega = 0 \qquad \mathbf{u} = \mathbf{K} * \omega, \tag{1}$$

where $\mathbf{K}(\mathbf{x}, \mathbf{y}) := \nabla^\perp \Delta_{\mathbb{T}}^{-1} \delta_{\mathbf{y}}(\mathbf{x})$ denotes the Biot-Savart kernel on the torus. The initial value problem is well-posed for every bounded initial datum

$$\omega^0(\mathbf{x}) \in L^\infty(\mathbb{T}^2)$$

and produces a unique solution $\omega \in L^\infty([0,\infty) \times \mathbb{T}^2)$ (see [58]). We will work in this setting.

The aim of this section is to rigorously prove some results concerning the dynamics of a concentrated blob of vorticity with respect to a shear flow with a non-zero vorticity gradient. Let $\bar{\omega}^0(\mathbf{x})$ be a steady smooth solution $\bar{\mathbf{u}}^0$ be the associated velocity field. This is equivalent (cf. (1)) to requiring that

$$\text{the vectors } \bar{\mathbf{u}}^0(\mathbf{x}) \text{ and } \nabla \bar{\omega}^0(\mathbf{x}) \text{ are orthogonal} \qquad \text{for every } \mathbf{x} \in \mathbb{T}^2. \tag{2}$$

A passive particle immersed in the fluid moves according to the differential equation $\dot{\mathbf{x}} = \bar{\mathbf{u}}^0(\mathbf{x})$. A point vortex with non-zero vorticity modifies the underlying vorticity field $\bar{\omega}^0$, so that its motion deviates from that of a passive particle. We want to describe this deviation, namely the motion along the direction perpendicular to $\bar{\mathbf{u}}^0(\mathbf{x})$, so parallel to $\nabla\bar{\omega}^0(\mathbf{x})$ (whenever this vector is non-zero).

To make our calculation rigorous we will not use the exact vortex-wave model (see the later Section 3), but instead a *blob-wave* system of equations, where we substitute the delta Dirac with a smooth, compactly supported function with a diameter of the support of order $\varepsilon \ll 1$. To be more precise, let $\mathbf{x}^0 \in \mathbb{T}^2$ (the center of the blob), $\Gamma \in \mathbb{R}$ (the circulation the blob) and $p(\mathbf{x}) \in C_c^\infty(\mathbb{R}^2)$ be a smooth function such that[1]

$$p \geq 0, \int p(\mathbf{x})dx = 1, \int \mathbf{x}\ p(\mathbf{x})dx = 0, \text{and} \operatorname{supp} p \subset B(0, \tfrac{1}{2}).$$

For $\varepsilon > 0$, define

$$\rho^{0,\varepsilon}(\mathbf{x}) = \Gamma p^\varepsilon(\mathbf{x}) := \frac{\Gamma}{\varepsilon^2} p\left(\frac{\mathbf{x}-\mathbf{x}^0}{\varepsilon}\right). \tag{3}$$

which will be the profile of a vortex around $\mathbf{x}^0$ with total circulation Γ. The blob-wave dynamics is the solution of the following problem

$$\begin{cases} \partial_t\bar{\omega} + \mathbf{u}\cdot\nabla\bar{\omega} = 0 & \bar{\omega}^{t=0}(\mathbf{x}) = \bar{\omega}^0(\mathbf{x}),\\ \partial_t\rho + \mathbf{u}\cdot\nabla\rho = 0 & \rho^{t=0}(\mathbf{x}) = \rho^{0,\varepsilon}(\mathbf{x})\\ \mathbf{u}^t(\mathbf{x}) = \int_{\mathbb{T}^d} \mathbf{K}(\mathbf{x},\mathbf{y})(\bar{\omega}^t(\mathbf{y}) + \rho^t(\mathbf{y}))dy \end{cases} \tag{4}$$

where $\bar{\omega}^t(\mathbf{x})$ and $\rho^t(\mathbf{x})$ describe respectively the evolution of the large-scale vorticity field $\bar{\omega}$ and of the vortex ρ. Summing the first two equations, we obtain that the total vorticity $\omega = \bar{\omega} + \rho$ solves the Euler Eq. (1) starting from the initial condition $\omega^0(\mathbf{x}) = \bar{\omega}^0(\mathbf{x}) + \rho^{0,\varepsilon}(\mathbf{x})$.

In [22] it is proven, in a slightly different setting, that the solutions of blob-wave dynamics converge (weakly as measures) to a solution of the vortex-wave system (Section 3), possibly allowing for a greater number of blobs, but with the additional assumption that the underlying vorticity field $\bar{\omega}^0$ is locally constant around the initial position of the blobs.

Following [22], we introduce the barycenter of the blob

$$\mathbb{T}^2 \ni \mathbf{G}(t) = \big(G_1(t), G_2(t)\big) := \int \mathbf{x}\ \rho^t(\mathbf{x})dx \Big/ \int \rho^t(\mathbf{x})dx = \frac{1}{\Gamma}\int \mathbf{x}\ \rho^t(\mathbf{x})dx.$$

Theorem 1. *Assume that*

$$\bar{\omega}^0(\mathbf{x}) \text{ depends only on } x_2 \qquad \text{and} \qquad \Gamma > 0,\ \partial_2\bar{\omega}^0(\mathbf{x}^0) > 0. \tag{5}$$

Then there exists a positive $\varepsilon_0 = \varepsilon_0(\bar{\omega}^0, \Gamma, p)$ and, for every $\varepsilon \in (0, \varepsilon_0]$, a time $T = T(\varepsilon) > 0$ such that $G_2(t)$ is stricly increasing in $[0, T]$. More precisely,

$$G_2'(0) = 0 \qquad \text{and} \qquad \left|G_2''(0) - \frac{\Gamma\partial_2\bar{\omega}^0(\mathbf{x}^0)}{4\pi}\ln\frac{1}{\varepsilon}\right| \lesssim_{\bar{\omega}^0, p} 1. \tag{6}$$

Proof. Introducing the velocity generated by the blob and the background vorticity respectively

$$\mathbf{v} := \mathbf{K} * \rho, \qquad \bar{\mathbf{u}} := \mathbf{K} * \bar{\omega}. \tag{7}$$

we have

$$\partial_t\bar{\omega}^{t=0}(\mathbf{x}) \overset{(1)}{=} -\bar{\mathbf{u}}^0(\mathbf{x})\cdot\nabla\bar{\omega}^0(\mathbf{x}) - \mathbf{v}^0(\mathbf{x})\cdot\nabla\bar{\omega}^0(\mathbf{x}) \overset{(2)}{=} -\mathbf{v}^0(\mathbf{x})\cdot\nabla\bar{\omega}^0(\mathbf{x})$$

hence

$$\partial_t\bar{\mathbf{u}}^{t=0}(\mathbf{x}) = \mathbf{K} * \partial_t\bar{\omega}^{t=0}(\mathbf{x}) = -\mathbf{K} * (\mathbf{v}^0\cdot\nabla\bar{\omega}^0)(\mathbf{x}). \tag{8}$$

Let us show the first item in (6). The first assumption in (5) is equivalent to

$$\bar{\mathbf{u}}^0(\mathbf{x}) = (\bar{u}_1^0(x_2), 0). \tag{9}$$

The velocity of the barycenter is

$$\mathbf{G}'(t) = \frac{1}{\Gamma}\int_{\mathbb{T}} \mathbf{x}\partial_t\rho dx = \frac{1}{\Gamma}\int_{\mathbb{T}} \rho(\bar{\mathbf{u}} + \mathbf{v})dx = \frac{1}{\Gamma}\int_{\mathbb{T}} \rho\bar{\mathbf{u}}dx, \tag{10}$$

where in the last equality we used the antisymmetry of $\mathbf{K}$ to deduce

$$\int \rho\mathbf{v}dx = \int \mathbf{K}(\mathbf{x},\mathbf{y})\rho(\mathbf{x})\rho(\mathbf{y})dxdy = 0.$$

Evaluating at $t = 0$ and using (9), we deduce $G_2'(0) = 0$.

Regarding the second derivative, let us start be showing that

$$G_2''(0) = \Gamma\int_{\mathbb{T}^2} \big(K_2 * p^\varepsilon(\mathbf{x})\big)^2\partial_2\bar{\omega}^0(\mathbf{x})dx. \tag{11}$$

Taking the derivative in (10), we get

$$\mathbf{G}''(t) = \frac{1}{\Gamma}\int \bar{\mathbf{u}}\partial_t\rho dx + \frac{1}{\Gamma}\int \rho\partial_t\bar{\mathbf{u}}dx.$$

Evaluating at time 0 and using (8), we have

$$\begin{aligned}\mathbf{G}''(0)\cdot\hat{\mathbf{x}}_2 &= \frac{\hat{\mathbf{x}}_2}{\Gamma}\cdot\int \rho^0\big(-\mathbf{K} * (\mathbf{v}^0\cdot\nabla\bar{\omega}^0)\big)dx = \frac{\hat{\mathbf{x}}_2}{\Gamma}\cdot\int (\mathbf{K} * \rho^0)(\mathbf{v}^0\cdot\nabla\bar{\omega}^0)dx\\ &\overset{(7)}{=} \frac{\hat{\mathbf{x}}_2}{\Gamma}\cdot\int \mathbf{v}^0(\mathbf{v}^0\cdot\nabla\bar{\omega}^0)dx \overset{(5)}{=} \frac{1}{\Gamma}\int (\mathbf{v}(0,\mathbf{x})\cdot\hat{\mathbf{x}}_2)^2\partial_2\bar{\omega}^0(\mathbf{x})dx.\end{aligned}$$

Using the definitions of $\mathbf{v}$ and $\boldsymbol{\rho}$ in (7) & (3), we obtain (11).

Let us identify the unit torus with $[-\frac{1}{2}, \frac{1}{2}]^2$ and assume without loss of generality that $\mathbf{x}^0 = 0$. Let us recall that the Biot-Savart kernel on the torus can be written as

$$K_2(\mathbf{x}) = \bar{K}_2(\mathbf{x}) + h(\mathbf{x}) \qquad \text{with} \qquad \bar{K}(\mathbf{x}) = \frac{\mathbf{x}^\perp}{2\pi|\mathbf{x}|^2}, h \in L^\infty(\mathbb{T}^2).$$

In order to exploit the better scaling properties of $\bar{K}$ with respect to K, let us show that

$$\left|\int_{\mathbb{T}^2}(K_2 * p^\varepsilon(\mathbf{x}))^2dx - \int_{\mathbb{T}^2}(\bar{K}_2 * p^\varepsilon(\mathbf{x}))^2dx\right| \lesssim 1. \tag{12}$$

This is a consequence of the following inequalities:

$$\begin{aligned}&\left|\int_{\mathbb{T}^2}\big(K_2 * p^\varepsilon(\mathbf{x})\big)^2\,dx - \int_{\mathbb{T}^2}\big(\bar{K}_2 * p^\varepsilon(\mathbf{x})\big)^2\,dx\right|\\ &\leq \int_{\mathbb{T}^2}\left|(K_2 + \bar{K}_2) * p^\varepsilon(\mathbf{x})\right|\left|(K_2 - \bar{K}_2) * p^\varepsilon(\mathbf{x})\right|dx\\ &\leq \left\|(K_2 + \bar{K}_2) * p^\varepsilon\right\|_{L^1(\mathbb{T}^2)}\left\|h * p^\varepsilon\right\|_{L^\infty(\mathbb{T}^2)}\\ &\leq \big(2\|\bar{K}_2\|_{L^1(\mathbb{T}^2)} + \|h\|_{L^1(\mathbb{T}^2)}\big)\|h\|_{L^\infty(\mathbb{T}^2)} \lesssim 1.\end{aligned}$$

As a second step, let us prove that

$$\left|\int_{\mathbb{T}^2}(\bar{K}_2 * p^\varepsilon(\mathbf{x}))^2\,dx - \frac{1}{4\pi}\ln\frac{1}{\varepsilon}\right| \lesssim 1. \tag{13}$$

The rescaling $\mathbf{x} \mapsto \mathbf{x}' := \varepsilon^{-1}\mathbf{x}$ and the (-1)-homogeneity of $\bar{K}_2$ yields the following

$$\begin{aligned}&\int_{\mathbb{T}^2}\big(\bar{K}_2 * p^\varepsilon(\mathbf{x})\big)^2\,dx\\ &\overset{(3)}{=} \int_{\mathbb{T}^2}\Big(\int_{\mathbb{R}^2}\bar{K}_2(\mathbf{x}-\mathbf{y})\frac{1}{\varepsilon^2}p\big(\frac{\mathbf{y}}{\varepsilon}\big)dy\Big)\Big(\int_{\mathbb{R}^2}\bar{K}_2(\mathbf{x}-\mathbf{z})\frac{1}{\varepsilon^2}p\big(\frac{\mathbf{z}}{\varepsilon}\big)dz\Big)dx\\ &= \int_{\frac{1}{\varepsilon}\mathbb{T}^2}\Big(\int_{\mathbb{R}^2}\varepsilon\bar{K}_2(\varepsilon(\mathbf{x}'-\mathbf{y}'))p(\mathbf{y}')d\mathbf{y}'\Big)\Big(\int_{\mathbb{R}^2}\varepsilon\bar{K}_2(\varepsilon(\mathbf{x}'-\mathbf{z}'))p(\mathbf{z}')\big)dz'\Big)dx'\\ &= \int_{\frac{1}{\varepsilon}\mathbb{T}^2}\Big(\int_{\mathbb{R}^2}\bar{K}_2(\mathbf{x}'-\mathbf{y}')p(\mathbf{y}')d\mathbf{y}'\Big)\Big(\int_{\mathbb{R}^2}\bar{K}_2(\mathbf{x}'-\mathbf{z}')p(\mathbf{z}')\big)dz'\Big)dx'\\ &= \int_{\frac{1}{\varepsilon}\mathbb{T}^2}\big(\bar{K}_2 * p(\mathbf{x})\big)^2\,dx.\end{aligned}$$

Splitting the domain of integration of the last integral, we get

$$\int_{B(0,2)}\big(\bar{K}_2 * p(\mathbf{x})\big)^2\,dx + \int_{\frac{1}{\varepsilon}\mathbb{T}^2\setminus B(0,2)}\big(\bar{K}_2 * p(\mathbf{x})\big)^2\,dx.$$

The first term is bounded by $\|\bar{K}_2\|_{L^1(B(0,2))}\|p\|_{L^\infty(B(0,2))} \lesssim 1$, so it is enough to study the second one. Up to an additive error of order 1, we can neglect the convolution since

$$\left|\int_{\frac{1}{\varepsilon}\mathbb{T}^2\setminus B(0,2)}\big(\bar{K}_2 * p(\mathbf{x})\big)^2\,dx - \int_{\frac{1}{\varepsilon}\mathbb{T}^2\setminus B(0,2)}\bar{K}_2(\mathbf{x})^2\,dx\right|$$

[1] by $dx := dx_1dx_2$ we mean the volume element of the torus.

$$\le \int_{\frac{1}{\varepsilon}\mathbb{T}^2\setminus B(0,2)} \Big(\int |\bar K_2(\mathbf{x}-\mathbf{y}) + \bar K_2(\mathbf{x})| p(\mathbf{y}) dy \Big) \Big(\int |\bar K_2(\mathbf{x}-\mathbf{y}) - \bar K_2(\mathbf{x})| p(\mathbf{y}) dy \Big) dx$$
$$\lesssim \int_{\frac{1}{\varepsilon}\mathbb{T}^2\setminus B(0,2)} \sup_{\mathbf{y}\in B(0,1)} |\bar K_2(\mathbf{x}-\mathbf{y})| \sup_{\mathbf{y}\in B(0,1)} |\nabla \bar K_2(\mathbf{x}-\mathbf{y})| dx$$
$$\lesssim \int_{\frac{1}{\varepsilon}\mathbb{T}^2\setminus B(0,2)} \sup_{\mathbf{y}\in B(0,1)} \frac{1}{|\mathbf{x}-\mathbf{y}|} \sup_{\mathbf{y}\in B(0,1)} \frac{1}{|\mathbf{x}-\mathbf{y}|^2} dx \lesssim \int_{\mathbb{R}^2\setminus B(0,2)} \frac{1}{|\mathbf{x}|^3} \lesssim 1,$$

so that (13) will be implied by

$$-1 \lesssim \int_{\frac{1}{\varepsilon}\mathbb{T}^2\setminus B(0,2)} \bar K_2(\mathbf{x})^2 \, dx - \frac{1}{4\pi}\ln\frac{1}{\varepsilon} \lesssim 1.$$

Using that $\mathbb{T}^2 \subset B(0, \frac{1}{\sqrt{2}})$, we deduce the upper bound (the lower bound follows analogously from $\mathbb{T}^2 \supset B(0, \frac{1}{2})$):

$$\int_{\frac{1}{\varepsilon}\mathbb{T}^2\setminus B(0,2)} \bar K_2(\mathbf{x})^2 \, dx \le \int_{B(0,\frac{1}{\sqrt{2}\varepsilon})\setminus B(0,2)} \bar K_2(\mathbf{x})^2 \, dx = \frac{1}{4\pi^2}\int_{B(0,\frac{1}{\sqrt{2}\varepsilon})\setminus B(0,2)} \frac{x_1^2}{|\mathbf{x}|^4} dx$$
$$= \frac{1}{8\pi^2}\int_{B(0,\frac{1}{\sqrt{2}\varepsilon})\setminus B(0,2)} \frac{x_1^2+x_2^2}{|\mathbf{x}|^4} dx$$
$$= \frac{1}{4\pi}\int_2^{\frac{1}{\sqrt{2}\varepsilon}} \frac{1}{\rho} d\rho = \frac{1}{4\pi}\ln\frac{1}{\varepsilon} + O(1).$$

From (12) and (13), we have proven that

$$\Big| \int_{\mathbb{T}^2} \big(K_2 * p^\varepsilon(\mathbf{x})\big)^2 \, dx - \frac{1}{4\pi}\ln\frac{1}{\varepsilon} \Big| \lesssim_p 1.$$

Starting from this and using (11), then (6) is finally established once we prove that

$$\Big| \int_{\mathbb{T}^2} \big(K_2 * p^\varepsilon(\mathbf{x})\big)^2 \partial_2\bar\omega^0(\mathbf{x}) dx - \partial_2\bar\omega^0(0)\int_{\mathbb{T}^2}\big(K_2 * p^\varepsilon(\mathbf{x})\big)^2 \, dx \Big| \lesssim \|\nabla^2\bar\omega^0\|_\infty,$$

which follows from the following sequence of inequalities

$$\int_{\mathbb{T}^2} \big(K_2 * p^\varepsilon(\mathbf{x})\big)^2 |\partial_2\bar\omega^0(\mathbf{x}) - \partial_2\bar\omega^0(0)| dx \lesssim \|\nabla^2\bar\omega^0\|_{L^\infty}\int_{\mathbb{T}^2} (K_2 * p^\varepsilon(\mathbf{x}))^2 |\mathbf{x}| dx$$
$$= \|\nabla^2\bar\omega^0\|_{L^\infty}\Big(\int_{B(0,2\varepsilon)} (K_2 * p^\varepsilon(\mathbf{x}))^2|\mathbf{x}|dx + \int_{\mathbb{T}^2\setminus B(0,2\varepsilon)} (K_2 * p^\varepsilon(\mathbf{x}))^2|\mathbf{x}|dx\Big)$$
$$\le \|\nabla^2\bar\omega^0\|_{L^\infty}\Big(\varepsilon\int_{B(0,2\varepsilon)} (K_2 * p^\varepsilon(\mathbf{x}))^2 \, dx + \int_{\mathbb{T}^2\setminus B(0,2\varepsilon)} (\sup_{B(0,\varepsilon)} |K_2(\mathbf{x}-\mathbf{y})|)^2|\mathbf{x}|dx\Big)$$
$$\lesssim \|\nabla^2\bar\omega^0\|_{L^\infty}\Big(\varepsilon\ln\frac{1}{\varepsilon} + \int_{\mathbb{T}^2\setminus B(0,2\varepsilon)} \frac{1}{|\mathbf{x}|^2}|\mathbf{x}|dx\Big) \lesssim \|\nabla^2\bar\omega^0\|_{L^\infty}.$$

□

Remark 2. From (6), one deduces that the general case (without making assumptions of the signs of Γ and $\partial_{x_2}\bar\omega^0(\mathbf{x}^0)$) is that the map

$$t \mapsto \operatorname{sign}\big(\Gamma\partial_2\bar\omega^0(\mathbf{x}^0)\big)G_2(t)$$

is strictly increasing.

Remark 3. Following the same lines of the proof above, the theorem can be extended in the following way. Assume $\bar\omega^0(\mathbf{x})$ is a steady solution of the Euler equations (not necessarily depending only on x_2). Without loss of generality, assume that $\Gamma > 0$ and that $\nabla\bar\omega^0(\mathbf{x}^0) = \partial_2\bar\omega^0(\mathbf{x}^0)\hat{\mathbf{x}}_2$ with $\partial_2\bar\omega^0(\mathbf{x}^0) > 0$ (cf. Remark 2 for the other cases). Call $\mathbf{G}^\varepsilon(t)$ the position of the barycentre depending on the parameter ε. Then

$$\lim_{\varepsilon\to 0} G_2^\varepsilon(0)' = 0 \qquad \lim_{\varepsilon\to 0} G_2^\varepsilon(0)'' = +\infty.$$

Since the second derivative is divergent in the limit $\varepsilon \to 0$, it is natural to ask whether the limiting behaviour of the point vortex is of the form

$$G_2(t) \sim t^\alpha \qquad \text{for some } \alpha \in (1,2).$$

We were unable to theoretically determine it, but we analysed the problem numerically both with the blob-wave dynamics with decreasing radius of the blob ε (Fig. 2) and the limiting vortex-wave system (Fig. 1). The time-scales at which we observe the fitting with the $\frac{3}{2}$ exponent in Fig. 1 differ by a factor 10 from Fig. 2. This is conceivable, as we are comparing a point-wise vortex with a blob of positive area. A precise description of the trajectory of the barycenter of the blob, in the limit of its size vanishing, is beyond the scope of this work and is left for a future study. We stress that the numerical simulations presented do not validate the theoretical predictions in a strict sense. Nevertheless, we show discrete agreement with the analysis performed in this section. We refer to the next section for a more detailed description of the numerical scheme used.

3. The vortex-wave system

3.1. The model

In this section, we recall the results of Marchioro and Pulvirenti about the vortex-wave system (see [22]). [2] Let us consider the incompressible Euler equations on the unit sphere $\mathbb{S}^2 \subset \mathbb{R}^3$

$$\partial_t\omega + \{\psi,\omega\} = 0 \qquad \Delta_{\mathbb{S}^2}\psi = \omega, \tag{14}$$

where $\omega, \psi : \mathbb{S}^2 \to \mathbb{R}$ denote respectively the (scalar) vorticity and the stream function and $\{\cdot,\cdot\}$ the Poisson brackets on the sphere. For a classical solution of (14), the velocity of the fluid $\mathbf{u}^t(\mathbf{x})$ defined by

$$\mathbf{u}^t(\mathbf{x}) = \nabla^\perp_{\mathbb{S}^2}\psi^t(\mathbf{x}) \in T_{\mathbf{x}}\mathbb{S}^2 \qquad \text{for } t \in [0,\infty) \text{ and } \mathbf{x} \in \mathbb{S}^2 \tag{15}$$

generates a flow of diffeomorphism $\Phi^t : \mathbb{S}^2 \to \mathbb{S}^2$ which satisfies

$$\Phi^0(\mathbf{x}) = \mathbf{x} \qquad \text{and} \qquad \partial_t\Phi^t(\mathbf{x}) = \mathbf{u}^t(\Phi^t(\mathbf{x})) \qquad \text{for all } t \in [0,\infty) \text{ and } \mathbf{x} \in \mathbb{S}^2,$$

and so that the transport formula $\omega^t(\mathbf{x}) = \omega^0\big((\Phi^t)^{-1}(\mathbf{x})\big)$ holds.

We will consider an initial condition ω^0 which is a (possibly signed) measure of the form

$$\omega^0(d\mathbf{x}) = \bar\omega^0(\mathbf{x})d\mathbf{x} + \Gamma\delta_{\mathbf{x}^0}(d\mathbf{x}),$$

where $\bar\omega^0 \in L^\infty(\mathbb{S}^2)$ denotes a large-scale background vorticity and $\Gamma\delta_{\mathbf{x}^0}$ a point-like vortex located at $\mathbf{x}^0 \in \mathbb{S}^2$ of circulation Γ. In [22], denoting, respectively, by $\bar\omega^t$ and $\mathbf{x}_v(t) \in \mathbb{S}^2$ the background vorticity and the position of the vortex at time t, the time-dependent measure

$$\omega^t(d\mathbf{x}) = \bar\omega^t(\mathbf{x})d\mathbf{x} + \Gamma\delta_{\mathbf{x}_v(t)}(d\mathbf{x})$$

is said to satisfy the Euler equations in a weak form if $\bar\omega \in L^\infty([0,+\infty)\times\mathbb{S}^2)$, $\mathbf{x}_v \in C^1([0,+\infty),\mathbb{S}^2)$ and the following system of equations holds

$$\begin{cases} \partial_t\Phi^t(\mathbf{x}) = \bar{\mathbf{u}}^t\big(\Phi^t(\mathbf{x})\big) + \Gamma\mathbf{K}\big(\Phi^t(\mathbf{x}),\mathbf{x}_v(t)\big), \quad \Phi^0(\mathbf{x}) = \mathbf{x},\ \mathbf{x} \ne \mathbf{x}^0 \\ \dfrac{d\mathbf{x}_v}{dt}(t) = \bar{\mathbf{u}}^t\big(\mathbf{x}_v(t)\big), \quad \mathbf{x}_v(0) = \mathbf{x}^0 \\ \bar{\mathbf{u}}^t(\mathbf{x}) = \displaystyle\int_{\mathbb{S}^2}\mathbf{K}(\mathbf{x},\mathbf{y})\bar\omega^t(\mathbf{y})dy \\ \bar\omega^t(d\mathbf{x}) = \bar\omega^0\big((\Phi^t)^{-1}(\mathbf{x})\big) \end{cases} \tag{16}$$

Here $\bar{\mathbf{u}}$ is the velocity field given by $\bar\omega$, the bounded part of the vorticity. In this section, the function $\mathbf{K} = \mathbf{K}_{\mathbb{S}^2}$ is the Biot-Savart kernel on $\mathbb{S}^2$

$$\mathbf{K}(\mathbf{x},\mathbf{y}) := \nabla^\perp_{\mathbb{S}^2}\Delta^{-1}_{\mathbb{S}^2}\delta_{\mathbf{y}}(\mathbf{x}) = \frac{1}{2\pi}\frac{(\mathbf{x}-\mathbf{y})\times\mathbf{y}}{|\mathbf{x}-\mathbf{y}|^2}.$$

The point vortex $\mathbf{x}_v$ follows only the velocity field $\bar{\mathbf{u}}$, discarding the self-interaction, while $\bar\omega$ evolves transported by the sum of the divergent velocity field of the vortex and its velocity field $\bar{\mathbf{u}}$.

Some results from [22] are summarised in the following theorem.

Theorem 4. *Given initial conditions $\bar\omega^0 \in L^\infty(\mathbb{S}^2)$, $\mathbf{x}^0 \in \mathbb{S}^2$ and $\Gamma \in \mathbb{R}\setminus\{0\}$, there exists a global in time solution of system (16). Under the additional assumption that $\bar\omega^0$ is constant in a neighbourhood of $\mathbf{x}^0$, the solution is unique and it is the weak-* limit (in the sense of finite measures) as $\varepsilon \downarrow 0$ of the solutions starting from the bounded initial conditions*

$$\omega^{0,\varepsilon}(\mathbf{x}) := \bar\omega^0(\mathbf{x}) + \frac{\Gamma}{\pi\varepsilon^2}\chi_{B(\mathbf{x}^0,\varepsilon)}$$

[2] For our later scopes, we give the results on $\mathbb{S}^2$, rather than $\mathbb{R}^2$. We have not seen any crucial difference in changing the reference domain to extend the results of [22].

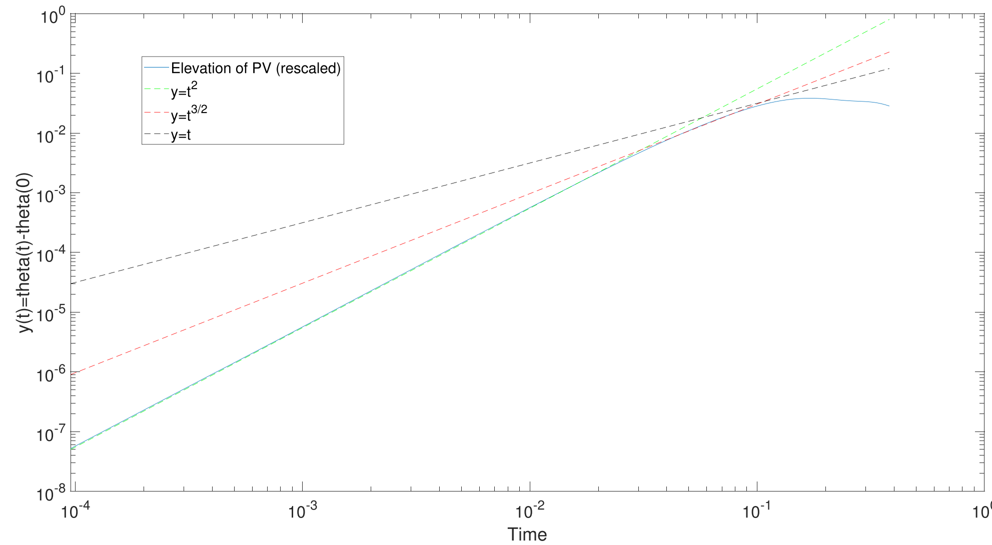

Fig. 1. Vertical coordinate trajectory $y = y(t) := \theta(0) - \theta(t)$, plotted in loglog scale, of a point-vortex x_v on a sphere in azimuth-inclination coordinates (φ, θ) with background vorticity ω equal to the Coriolis vorticity. The plot is obtained by a DNS of (18) via the numerical scheme described at the end of Section 3, for $N = 65$ and time-step $h = 10^{-5}$. The point-vortex has circulation $\Gamma = 0.1$, initial inclination $\theta(0) = \pi - \arccos 0.6$, the Coriolis vorticity is $f = 62\cos\theta$. In the very initial time, of approximately $10^{-2}s$, the slope of the curve is approximately 2. After that, it bends towards $\frac{3}{2}$, which would fit with the prediction of Remark 3 of the second derivative being infinity at $t = 0$. However, the time where the slope is $\frac{3}{2}$ is comparable to the one in which it is 2. Therefore this simulation cannot be conclusive. After $0.1s$ the trajectory of the vortex stops to follow any power law in time, due to the emergence of some more complex dynamics.

where $\chi_{B(\mathbf{x}^0,\varepsilon)}$ denotes the characteristic function of the ball $B(\mathbf{x}^0, \varepsilon)$ centered at $\mathbf{x}^0$ of radius ε.

Due to the divergence of the vector field of the vortex, the case when $\bar\omega^0$ is not locally constant is less understood. In the smooth case, $\bar\omega^0$ is not locally constant in particular if $\nabla\bar\omega^0(\mathbf{x}^0) \neq 0$. Under this assumption, we provide numerical simulations (Section 3.2) and a rigorous proof (Section 2) that the vortex perceives a very strong acceleration proportional to $\Gamma\nabla\bar\omega(\mathbf{x}^0)$.

3.2. Direct numerical simulations

In this section, we specifiy the vortex-wave Eq. (16) on a rotating 2-sphere $\mathbb{S}^2 \subset \mathbb{R}^3$. These equations were first introduced by Bogomolov [59] and more recently studied by Laurent–Polz in [60], in the context of geometric mechanics. Formally, we set the equations in the following notations:

- Position of the point vortices: $\mathbf{x}_v^i : [0, T] \to \mathbb{S}^2$, for $i = 1, \ldots, N_V$.
- Background vorticity: $\bar\omega : [0, T] \times \mathbb{S}^2 \to \mathbb{R}$.
- *Coriolis vorticity*: $f = f(\mathbf{x}) := \mathbf{\Omega} \cdot \mathbf{x}$, for $\mathbf{\Omega} \in \mathbb{R}^3$ angular velocity of the rotating sphere.

Then the vortex-wave equations on a rotating sphere are given by:

$$\begin{aligned} \dot{\mathbf{x}}_v^i &= \frac{1}{4\pi} \sum_{\substack{j=1,..,N_V\\ i\neq j}} \Gamma_j \frac{\mathbf{x}_v^i \times \mathbf{x}_v^j}{1 - \mathbf{x}_v^i \cdot \mathbf{x}_v^j} + \mathbf{x}_v^i \times \nabla\Delta_{\mathbb{S}^2}^{-1}(\bar\omega - f)(\mathbf{x}_v^i) \qquad \text{for } i = 1, \ldots, N_V \\ \dot{\bar\omega} &= \{\bar\omega, \Delta_{\mathbb{S}^2}^{-1}(\bar\omega - f) + \sum_{i=1,\ldots,N_V} \Gamma_i \log(1 - \mathbf{x}_v^i \cdot \mathbf{x})\}. \end{aligned} \tag{17}$$

The Poisson bracket of two functions f, g is defined as $\{f, g\} := \mathbf{x} \cdot (\nabla f \times \nabla g)$. We remark that the Laplace-Beltrami operator on the sphere $\Delta_{\mathbb{S}^2}$ is invertible on the space of functions with zero mean. Eq. (17) are a infinite dimensional Hamiltonian system (more precisely Lie–Poisson system) with energy

$$H = -\frac{1}{2}\sum_{i\neq j} \Gamma_i\Gamma_j \log(1 - \mathbf{x}_v^i \cdot \mathbf{x}_v^j) - \sum_i \Gamma_i(\bar\omega - f)(\mathbf{x}_v^i) - \frac{1}{2}\int_{\mathbb{S}^2} \Delta_{\mathbb{S}^2}^{-1}(\bar\omega - f)(\bar\omega - f).$$

Eq. (17) also have additional Casimir invariants given by $C_f = \int_{\mathbb{S}^2} f(\bar\omega)$, for any real function f and the angular momentum $M = \int_{\mathbb{S}^2}(\sum_i \Gamma_i \delta_{\mathbf{x}_v^i} + \bar\omega)\mathbf{n}\, dS \cdot \mathbf{\Omega}$, for $\mathbf{\Omega} \neq 0$.

A spatial discretization which retains many conservation laws is known for the 2D Euler equations as the Zeitlin model [61]. In the following discussions, we use the conventions of [62]. Starting from Eq. (17), we obtain the vortex-wave–Zeitlin model. Given the expansion of the vorticity field in spherical harmonics Y_{lm}, we take the truncated expansion for $l \leq N - 1, m = -l, \ldots, l$. Then, for any $N \geq 1$, we have an explicit vector space isomorphism between the one spanned by classical spherical harmonics $\{Y_{lm}\}_{\substack{l=1,..,N-1\\ m=-l,\ldots,l}}$ and a $\mathfrak{su}(N)$ (skew-Hermitian matrix with zero trace), spanned by the matrices $\{T_{lm}\}_{\substack{l=1,..,N-1\\ m=-l,\ldots,l}}$. In other words, if $\bar\omega = \sum_{l=1}^{\infty}\sum_{m=-l}^{l} \bar\omega^{lm} Y_{lm}$, then $W = \sum_{l=1}^{N-1}\sum_{m=-l}^{l} \bar\omega^{lm} T_{lm}$. In these notations, the vortex-wave–Zeitlin is given by:

$$\begin{aligned} \dot{\mathbf{x}}_v^i &= \frac{1}{4\pi} \sum_{\substack{j=1,..,N_V\\ i\neq j}} \Gamma_i \frac{\mathbf{x}_v^i \times \mathbf{x}_v^j}{1 - \mathbf{x}_v^i \cdot \mathbf{x}_v^j} \\ &\quad - \sum_{\substack{l=1,..,N-1\\ m=-l,\ldots,l}} \frac{\mathbf{x}_v^i \times \nabla Y_{lm}(\mathbf{x}_v^i)}{-l(l+1)} (W - F)^{lm} \qquad \text{for } i = 1, \ldots, N_V \\ \dot W &= -[W, \Delta_N^{-1}\big(W + \sum_{\substack{i=1,..,N_V\\ l=1,..,N-1\\ m=-l,\ldots,l}} \Gamma_i Y_{lm}(\mathbf{x}_v^i) T_{lm} - F\big)]_N, \end{aligned} \tag{18}$$

where Δ_N is the discrete Laplacian, $[A, B]_N = \frac{\sqrt{N^2-1}}{2}(AB - BA)$ and $F = |\mathbf{\Omega}| i T_{10}$. The Hamiltonian is:

$$\begin{aligned} H = \; & -\frac{1}{8\pi} \sum_{\substack{i,j=1,..,N_V\\ i\neq j}} \Gamma_i\Gamma_j \log(1 - \mathbf{x}_i \cdot \mathbf{x}_j) + \\ & - \sum_{\substack{i=1,..,N_V\\ l=1,..,N-1\\ m=-l,\ldots,l}} \Gamma_i \frac{Y_{lm}(\mathbf{x}_i)}{-l(l+1)} (W - F)^{lm} + \\ & -\frac{1}{2}\operatorname{Tr}(\Delta_N^{-1}(W - F)^*(W - F)). \end{aligned} \tag{19}$$

Eq. (18) have the following independent first integrals:

$$C_n(W) = \operatorname{Tr}(W^n), \text{ for } n = 2, \ldots, N - 1$$

$$M = \left(\sum_{i=1}^{N_V} \Gamma_i \mathbf{x}_v^i + \begin{bmatrix} \operatorname{Tr}(W^* T_x) \\ \operatorname{Tr}(W^* T_y) \\ \operatorname{Tr}(W^* T_z) \end{bmatrix} \right) \cdot \mathbf{\Omega}, \tag{20}$$

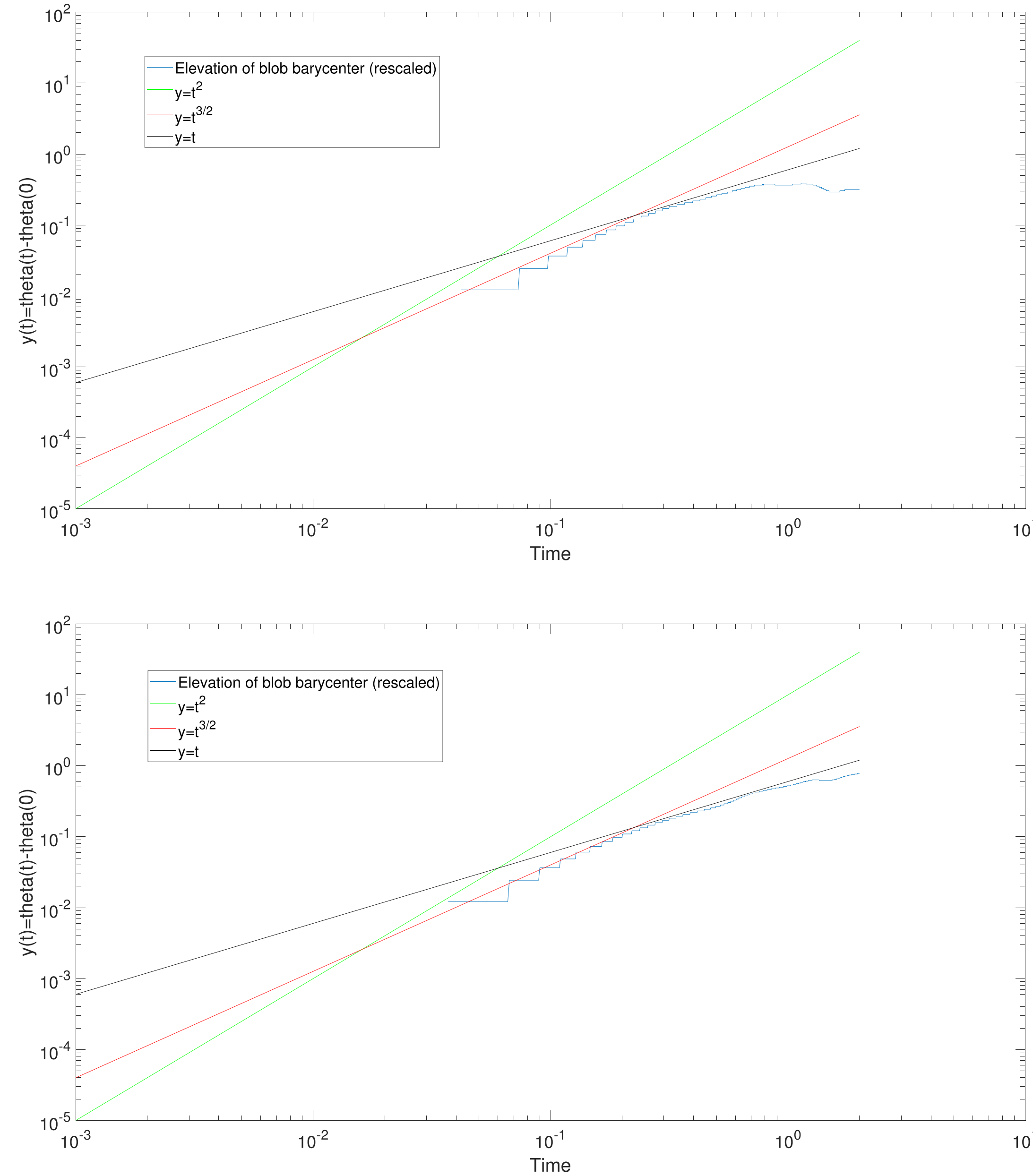

Fig. 2. Vertical coordinate trajectory $y = y(t) := \theta(0) - \theta(t)$, plotted in loglog scale, of the barycenter of a blob of vorticity ω_b of radius 10ϵ (top) and ϵ (bottom), on a sphere in azimuth-inclination coordinates (φ, θ) with background vorticity ω_r equal to the Coriolis vorticity in the simulation of Fig. 1. The blob is defined as in (3) and it has the same circulation and initial barycenter inclination coordinate of the point-vortex in the simulation of Fig. 1. The curve $y = y(t)$ is obtained by a DNS of (18) via the numerical scheme described at the end of Section 3, for $N = 257$, $\epsilon = 1/N$ and time-step $h = 10^{-3}$, with no point-vortices ($N_V = 0$) and with initial vorticity obtained by the discretization of $\omega = \omega_b + \omega_r$. The slope of the curve, after an initial short time, not captured by the tracking of the blob's barycenter, is around $\frac{3}{2}$, until we see a linear growth. We do not see significant differences between the two simulations, denoting a certain stability with respect to the blob size.

where $T_x = \frac{iT_{1-1} - iT_{1-1}}{\sqrt{2}}, T_y = \frac{T_{1-1} + T_{1-1}}{\sqrt{2}}, T_z = iT_{10}$.

A conservative time-discretization of Eq. (18) can be obtained by extending the method used in [63][3] to the coupled vortex-wave system. Therefore, we obtain a Lie–Poisson integrator for (18) that exactly conserves the integrals C_n and M and nearly conserves the Hamiltonian H. In Fig. 3, we illustrate an example of a DNS of (18), solved with the Lie–Poisson integrator developed in [63], in which 6 identical point-vortices are placed in the vertices of a regular equatorial hexagon and a background smooth vorticity equal to the Coriolis one.

[3] The code used to perform numerical simulations of the Zeitlin model can be found https://github.com/klasmodin/quflow. The code for the vortex-wave Zeitlin model is not available yet.

4. Quasi-two-dimensional flows

Most real systems where, in a first approximation a 2D model is investigated, are indeed quasi-two-dimensional. The deviation from 2D may be relevant and the consequences very important. We address to [33] for a review of problems and results on this topic.

The question we discuss in this section is whether our first-stage result of motion along the gradient extends to thin vortex tubes in 3D shear flows, with approximate symmetries that make the system close to 2D.

The first difficulty in order to develop a theory is the concept of *vortex tube* and its evolution. See [64] as an instance of the difficulty to handle this topic. Just to mention a technical problem we encountered when trying to extend our 2D result, the concept of center of mass $\mathbf{G}(t)$

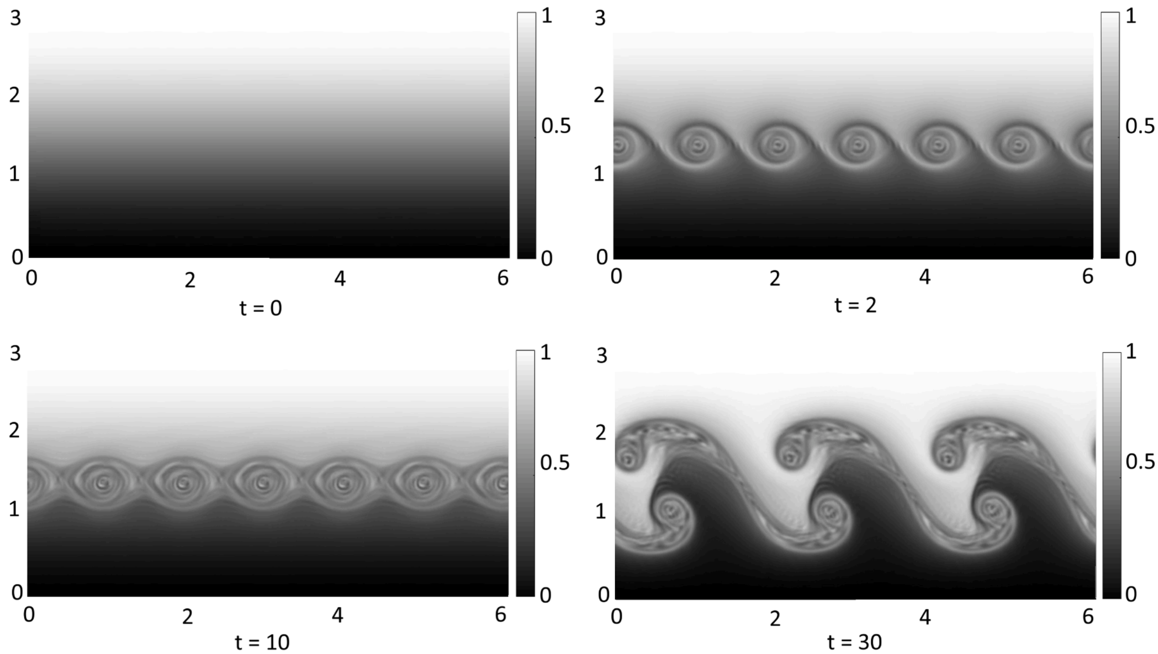

Fig. 3. From the top-left to the bottom-right, time snapshots of the evolution of the vorticity field ω on a 2-sphere, interacting with six equal equatorial point vortices. The plots, in azimuth-inclination coordinates (φ, θ), are obtained by a DNS of (18) for $N = 501$. The initial (unstable) equilibrium of 6 equatorial point-vortices placed at the vertices of a regular equatorial hexagon, all with the same vorticity $\Gamma > 0$, surrounded by an initial smooth field equal to the Coriolis vorticity $\omega^0 = 2\Omega\cos\theta$, for $\Omega = -1/2$, evolves into a coupled vortex-wave dynamics. Here, the self-interaction among the point-vortices is crucial to develop this kind of behaviour. The interaction with the background shear flow acts only as a perturbation of the initial equilibrium configuration of point-vortices.

introduced above is not very clear. Can we define a curve inside the vortex tube which replaces the center of mass?

What is easy to define is the concept of *vortex filament*: a time-dependent parametrized curve of the form

$$\boldsymbol{\gamma}^t(r) \in \mathbb{R}^3, \qquad r \in \mathbb{R}$$

where t is time and r is the parameter. Given a circulation parameter Γ, we may define the associated vorticity field as the vector valued distribution [65]

$$\boldsymbol{\omega}'(t,\mathbf{x}) = \Gamma \int_{\mathbb{R}} \delta\left(\mathbf{x} - \boldsymbol{\gamma}^t(r)\right)\partial_r \boldsymbol{\gamma}^t(r)\,dr$$

(we use the notation $\boldsymbol{\omega}'$ as if it were a fluctuation, a perturbation of a field). We may also create at time $t = 0$ a smoother version by a convolution

$$\boldsymbol{\omega}'_\varepsilon(0,\mathbf{x}) = \Gamma \int_{\mathbb{R}} p^\varepsilon\left(\mathbf{x} - \boldsymbol{\gamma}^0(r)\right)\partial_r \boldsymbol{\gamma}^0(r)\,dr$$

where $p^\varepsilon(\mathbf{x}) := \varepsilon^{-3}p\left(\varepsilon^{-1}\mathbf{x}\right)$ and p is a smooth compact support function of integral 1. However, opposite to the fact that the filament remains a curve for larger times, what happens to $\boldsymbol{\omega}'_\varepsilon(0,\mathbf{x})$ is less easy to describe. Also an initially circular blob in 2D is subject to strong deformations as time evolves, but at least we may investigate its baricenter. In the case of a vortex tube, this is more difficult.

One is therefore tempted to work with only the vortex filament, and investigate its evolution in a background shear flow. However, as explained in [65,66] and other works, the dynamics of a vortex filament is too singular and the only way to study it is by introducing a regularization (a cut-off) of the Biot-Savart kernel.

In the next two subsections, we proceed in this way, by mollification of the Biot-Savart kernel. We start in Section 4.1, working on the torus $\mathbb{T}^3$, with a slightly tilted vortex filament. In Section 4.2, we derive the result for a thin three-dimensional domain $\mathbb{T}^3_\delta$.

4.1. A vortex filament in a smoothed Biot-Savart set-up

Given a smooth $\alpha : \mathbb{T} \to \mathbb{T}$, let us consider an initial vortex filament in the three dimensional torus $\mathbb{T}^3$

$$\gamma^0 : \mathbb{T} \to \mathbb{T}^3, \qquad \gamma^0(r) = \alpha(r)\hat{\mathbf{x}}_2 + r\hat{\mathbf{x}}_3, \tag{21}$$

whose maximal slope with respect to the vertical line is described by the non-dimensional parameter

$$\eta := \|\alpha'(r)\|_\infty. \tag{22}$$

We will work in the regime $\eta \ll 1$, namely the vortex filament is just slightly tilted with respect to the vertical axis.

The velocity and the vorticity of the background shear flow are assumed to be of the form

$$\bar{\mathbf{u}}^0(\mathbf{x}) := (\bar{u}^0_1(x_2), 0, 0) \qquad \text{and} \qquad \bar{\omega}^0(\mathbf{x}) := (0, 0, \bar{\omega}^0_3(x_2)), \tag{23}$$

so that from the relation $\bar{\omega} = \operatorname{curl}\bar{u}$, we learn that

$$\bar{\omega}^0_3(x_2) = -\frac{d}{dx_2}\bar{u}^0_1(x_2). \tag{24}$$

Let us denote by $\mathbf{k}$ the Biot-Savart kernel on the torus $\mathbb{T}^3$ (identified in the sequel with $[-\frac{1}{2},\frac{1}{2}]^3$) and recall the following property

$$\mathbf{k}(\mathbf{x}) = \bar{\mathbf{k}}(\mathbf{x}) + \mathbf{h}(\mathbf{x}), \quad \text{with } \bar{\mathbf{k}}(\mathbf{x}) = \frac{1}{4\pi}\frac{\mathbf{x}}{|\mathbf{x}|^3} \text{ and } \mathbf{h} \in C^\infty\left([-\frac{1}{2},\frac{1}{2}]^3, \mathbb{R}^3\right).$$

We will use the regularized version $\mathbf{k}^\varepsilon$ of $\mathbf{k}$ defined by

$$\mathbf{k}^\varepsilon(\mathbf{x}) := \frac{1}{4\pi}\frac{\mathbf{x}}{(|\mathbf{x}|^2+\varepsilon^2)}^{\frac{3}{2}} + \mathbf{h}^\varepsilon(\mathbf{x}).$$

Here $\mathbf{h}_\varepsilon$ is a slight perturbation of $\mathbf{h}$ which makes the kernel $\mathbf{k}^\varepsilon$ periodic. We will only use that is satisfies uniform (in ε) L^∞ bounds.

The dynamics is the following

$$\partial_t\bar{\omega} + (\mathbf{u}+\mathbf{v})\cdot\nabla\bar{\omega} - \bar{\omega}\cdot\nabla(\mathbf{u}+\mathbf{v}) = 0, \tag{25}$$

$$\bar{\mathbf{u}}^t(\mathbf{x}) = \int_{\mathbb{T}^3} \mathbf{k}^\varepsilon(\mathbf{x}-\mathbf{y}) \times \bar{\omega}^t(\mathbf{y})\,dy, \tag{26}$$

$$\mathbf{v}^t(\mathbf{x}) = \Gamma \int_{\mathbb{T}} \mathbf{k}^\varepsilon(\mathbf{x} - \gamma^t(r)) \times \partial_r \gamma^t(r) dr, \tag{27}$$

$$\partial_t \gamma^t(r) = \bar{\mathbf{u}}^t(\gamma^t(r)) + \mathbf{v}^t(\gamma^t(r)). \tag{28}$$

The main result of this section is the following.

Theorem 5. *Assume that $\partial_2 \bar{\omega}_3^0(\gamma^0(r_0)) > 0$ for some $r_0 \in \mathbb{T}$. For $\bar{\omega}^0$ fixed, in the limit*

$$\varepsilon \ll 1 \qquad \text{and} \qquad \eta \ll \varepsilon^3 \frac{\partial_2 \bar{\omega}_3^0(\gamma^0(r_0))}{\Gamma}, \tag{29}$$

we have that

$$\partial_t \gamma_2^{t=0}(r_0) = 0 \qquad \text{and} \qquad \partial_t^2 \gamma_2^{t=0}(r_0) \sim \frac{\Gamma \partial_2 \bar{\omega}_3^0(\gamma^0(r_0))}{4\pi} \ln \frac{1}{\varepsilon}.$$

To do the proof, we need some technical lemmas. The first two give estimates on the regularized Biot-Savart kernel.

Lemma 6.

$$\int_{\mathbb{T}} \left| \partial_i k_j^\varepsilon(\gamma^0(r_0) - \gamma^0(r)) \right| dr \lesssim \varepsilon^{-2}, \tag{30}$$

$$\int_{\mathbb{T}} \left| \partial_i k_j^\varepsilon(\gamma^0(r_0) - \gamma^0(r)) \right| |r_0 - r| dr \lesssim \varepsilon^{-1}, \tag{31}$$

$$\int_{\mathbb{T}} \left| k_3^\varepsilon(\gamma^0(r_0) - \gamma^0(r)) \right| dr \lesssim \varepsilon^{-1}. \tag{32}$$

Proof. Let us show (30), since the other two are analogous. From the explicit expression

$$\partial_i k_j^\varepsilon(\mathbf{x}) = \delta_{ij}(|\mathbf{x}|^2 + \varepsilon^2)^{-\frac{3}{2}} - 3x_i x_j (|\mathbf{x}|^2 + \varepsilon^2)^{-\frac{5}{2}} + \partial_i h_j^\varepsilon$$

we learn that $|\partial_i k_j^\varepsilon|(\mathbf{x}) \lesssim (|\mathbf{x}|^2 + \varepsilon^2)^{-\frac{3}{2}}$. This implies

$$\begin{aligned} \int_{\mathbb{T}} \left| \partial_i k_j^\varepsilon(\gamma^0(r^0) - \gamma^0(r)) \right| dr &\lesssim \int_{\mathbb{T}} (|\gamma^0(r_0) - \gamma^0(r)|^2 + \varepsilon^2)^{-\frac{3}{2}} dr \leq \int_{\mathbb{T}} ((r - r_0)^2 + \varepsilon^2)^{-\frac{3}{2}} dr \\ &\lesssim \int_{|r-r_0| \geq \varepsilon} (r - r_0)^{-3} dr + \int_{|r-r_0| \leq \varepsilon} \varepsilon^{-3} dr \lesssim \varepsilon^{-2}. \end{aligned} \tag{33}$$

□

Lemma 7. *There exists a function $\phi : [0, \infty) \to [0, \infty)$ and a constant $C > 0$ with the properties*

$$\phi \text{ is increasing}, \qquad \phi(t) \leq Ct, \qquad \lim_{t \to \infty} \phi(t) = 1, \tag{34}$$

such that the following expansion holds

$$k_1^\varepsilon * k_1^\varepsilon(\mathbf{x}) = -\frac{1}{4\pi|\mathbf{x}|} \phi(\varepsilon^{-1}|\mathbf{x}|) + O(1) \qquad \text{for all } \mathbf{x} = (0, x_2, x_3).$$

Proof. Up to losing an error of order 1, we can prove the expansion for $\bar{k}_1^\varepsilon$ (in place of k_1^ε), for which we have

$$\bar{k}_1^\varepsilon * \bar{k}_1^\varepsilon(\mathbf{x}) = \frac{1}{16\pi^2} \int_{\mathbb{T}^3} \frac{x_1 - y_1}{(|\mathbf{x} - \mathbf{y}|^2 + \varepsilon^2)}^{\frac{3}{2}} \frac{y_1}{(|\mathbf{y}|^2 + \varepsilon^2)}^{\frac{3}{2}} dy.$$

With the identification $\mathbb{T}^3 \simeq [-\frac{1}{2}, \frac{1}{2}]^3$ and for $\mathbf{x} \in B(0, \frac{1}{4})$, we can extend the integral to the all space $\mathbb{R}^3$, by making an error of order one, since

$$\left| \int_{\mathbb{R}^3 \setminus [-\frac{1}{2}, \frac{1}{2}]^3} \frac{x_1 - y_1}{(|\mathbf{x} - \mathbf{y}|^2 + \varepsilon^2)}^{\frac{3}{2}} \frac{y_1}{(|\mathbf{y}|^2 + \varepsilon^2)}^{\frac{3}{2}} dy \right| \lesssim \int_{\mathbb{R}^3 \setminus [-\frac{1}{2}, \frac{1}{2}]^3} \frac{1}{|\mathbf{y}|^4} dy \lesssim 1$$

where in the first inequality we compared with $\varepsilon = 0$ and used that

$$|\mathbf{x} - \mathbf{y}| \geq \frac{1}{2}|\mathbf{y}| \qquad \text{for all } \mathbf{x} \in B(0, \frac{1}{4}), \mathbf{y} \in \mathbb{R}^3 \setminus [-\frac{1}{2}, \frac{1}{2}]^3.$$

If $x_1 = \mathbf{x} \cdot \hat{\mathbf{x}}_1 = 0$, then

$$\begin{aligned} \bar{k}_1^\varepsilon * \bar{k}_1^\varepsilon(\mathbf{x}) &= -\frac{1}{16\pi^2} \int_{\mathbb{R}^3} \frac{y_1^2}{(|\mathbf{x} - \mathbf{y}|^2 + \varepsilon^2)}^{\frac{3}{2}} (|\mathbf{y}|^2 + \varepsilon^2)^{\frac{3}{2}} dy + O(1) \\ &= -\frac{1}{16\pi^2} \int_{\mathbb{R}^3} \frac{y_1^2}{(|\mathbf{y} - |\mathbf{x}|\hat{\mathbf{x}}_3|^2 + \varepsilon^2)}^{\frac{3}{2}} \\ &\quad \times (|\mathbf{y}|^2 + \varepsilon^2)^{\frac{3}{2}} dy + O(1) \qquad \text{(Rotation in the } \hat{\mathbf{x}}_2, \hat{\mathbf{x}}_3 \text{ plane.)} \\ &= -\frac{1}{16\pi^2|\mathbf{x}|} \int_{\mathbb{R}^3} \frac{y_1^2}{(|\mathbf{y} - \hat{\mathbf{x}}_3|^2 + (\frac{\varepsilon}{|\mathbf{x}|})^2)}^{\frac{3}{2}} \\ &\quad \times (|\mathbf{y}|^2 + (\frac{\varepsilon}{|\mathbf{x}|})^2)^{\frac{3}{2}} dy + O(1) \qquad \text{(Change of variables } \mathbf{y} \mapsto |\mathbf{x}|\mathbf{y}.) \\ &= -\frac{1}{4\pi|\mathbf{x}|} \phi(\varepsilon^{-1}|\mathbf{x}|) + O(1), \end{aligned}$$

where we introduced

$$\phi(t) := \frac{1}{4\pi} \int_{\mathbb{R}^3} \frac{y_1^2}{(|\mathbf{y} - \hat{\mathbf{x}}_3|^2 + t^{-2})}^{\frac{3}{2}} (|\mathbf{y}|^2 + t^{-2})^{\frac{3}{2}} dy.$$

It remains to show (34). The monotonicity follows from the definition, while the limit at infinity follows from the explicit integral

$$\int_{\mathbb{R}^3} \frac{y_1^2}{|\mathbf{y} - \hat{\mathbf{x}}_3|^3 |\mathbf{y}|^3} dy = 4\pi.$$

Regarding the linear bound in t, it is enough to prove it for $t < \frac{1}{2}$, for which we have

$$\begin{aligned} \phi(t) &\lesssim \int_{B(0,t^{-1})} \frac{y_1^2}{(|\mathbf{y} - \hat{\mathbf{x}}_3|^2 + t^{-2})}^{\frac{3}{2}} (|\mathbf{y}|^2 + t^{-2})^{\frac{3}{2}} dy \\ &\quad + \int_{B(0,t^{-1})^c} \frac{y_1^2}{(|\mathbf{y} - \hat{\mathbf{x}}_3|^2 + t^{-2})}^{\frac{3}{2}} (|\mathbf{y}|^2 + t^{-2})^{\frac{3}{2}} dy \\ &\lesssim t^6 \int_{B(0,t^{-1})} |\mathbf{y}|^2 dy + \int_{B(0,t^{-1})^c} |\mathbf{y}|^{-4} dy \lesssim t. \end{aligned}$$

□

Now comes a lemma which exploits two quasi-two-dimensionality to derive estimates on the velocity field generated by the vortex filament.

Lemma 8.

$$\sup_{r \in \mathbb{T}} |v_1^0(\gamma^0(r))| \lesssim \Gamma \eta \varepsilon^{-1} \tag{35}$$

$$\sup_{\mathbf{x} \in \mathbb{T}^3} |\partial_3 \mathbf{v}^0(\mathbf{x})| \lesssim \Gamma \eta \varepsilon^{-2}. \tag{36}$$

Proof. From (21) and (27), we have that

$$v_1^0(\gamma^0(r)) = \Gamma \int_{\mathbb{T}} k_2^\varepsilon(\gamma^0(r) - \gamma^0(r')) dr' - \Gamma \int_{\mathbb{T}} \alpha'(r') k_3^\varepsilon(\gamma^0(r) - \gamma^0(r')) dr'.$$

The second term is estimated by (32) and definition (22). For the second term, we notice that

$$\left| k_2^\varepsilon(\gamma^0(r) - \gamma^0(r')) \right| \lesssim \frac{|\gamma_2(r) - \gamma_2(r')|}{(|r - r'|^2 + \varepsilon^2)}^{\frac{3}{2}} \lesssim \eta(|r - r'|^2 + \varepsilon^2)^{-1},$$

and apply the splitting $\mathbb{T} = \{|r - r'| \geq \varepsilon\} \cup \{|r - r'| < \varepsilon\}$ as in (33). This proves (35).

Regarding (36), we have

$$\begin{aligned} \partial_3 \mathbf{v}(\mathbf{x}) &= \Gamma \int_{\mathbb{T}} \partial_3 \mathbf{k}^\varepsilon(\mathbf{x} - \gamma^0(r)) \times \partial_r \gamma^0(r) dr = \\ &= \Gamma \int_{\mathbb{T}} \partial_3 \mathbf{k}^\varepsilon(\mathbf{x} - \gamma^0(r)) \times \alpha'(r) \hat{\mathbf{x}}_2 dr + \Gamma \int_{\mathbb{T}} \partial_3 \mathbf{k}^\varepsilon(\mathbf{x} - \gamma^0(r)) \times \hat{\mathbf{x}}_3 dr. \end{aligned}$$

The first term is estimated (up to a constant) by $\Gamma \eta \varepsilon^{-2}$ using (30) and $|\alpha'(r)| \leq \eta$. Finally, the same can be applied to the second one after observing that

$$\begin{aligned} \Gamma \int_{\mathbb{T}} \partial_3 \mathbf{k}^\varepsilon(\mathbf{x} - \gamma^0(r)) \times \hat{\mathbf{x}}_3 dr &= -\Gamma \int_{\mathbb{T}} \frac{d}{dr} \mathbf{k}^\varepsilon(\mathbf{x} - \gamma^0(r)) \times \hat{\mathbf{x}}_3 dr \\ &\quad - \Gamma \int_{\mathbb{T}} \partial_2 \mathbf{k}^\varepsilon(\mathbf{x} - \gamma^0(r)) \alpha'(r) \times \hat{\mathbf{x}}_3 dr \\ &= -\Gamma \int_{\mathbb{T}} \partial_2 \mathbf{k}^\varepsilon(\mathbf{x} - \gamma^0(r)) \alpha'(r) \times \hat{\mathbf{x}}_3 dr. \end{aligned}$$

□

We are finally able to show the theorem.

Proof of Theorem 5. Taking the time derivative of (28), we obtain

$$\partial_t^2 \gamma_2^{t=0}(r_0) = (\nabla \bar{u}_2)^{t=0}(\gamma^0(r_0)) \cdot \partial_t \gamma^{t=0}(r_0) + \partial_t (v_2^t(\gamma^t(r_0)))\Big|_{t=0} + (\partial_t \bar{u}_2)^{t=0}(\gamma^0(r_0))$$

The first term vanishes since $\bar{u}_2^0 \equiv 0$. The second one satisfies the estimate

$$|\partial_t(v_2^t(\gamma^t(r_0))\big|_{t=0}| \lesssim \eta\Big(\frac{\Gamma^2}{\varepsilon^3} + \frac{\Gamma\|\bar{\omega}^0\|_\infty}{\varepsilon}\Big), \tag{37}$$

which will be proven in the sequel. We can then discard it due to (29).

The main contribution will come from the last term, for which we have that

$$\begin{aligned}(\partial_t \bar{u}_2)^{t=0}(\gamma^0(r_0)) &\overset{(26)}{=} -\int_{\mathbb{T}^3} (\mathbf{k}^\varepsilon(\gamma^0(r_0)-\mathbf{y})\times\hat{\mathbf{x}}_2)\cdot(\partial_t\bar{\omega})^{t=0}(\mathbf{y})dy\\ &\overset{(25)}{=} \int_{\mathbb{T}^3} (\mathbf{k}^\varepsilon(\gamma^0(r_0)-\mathbf{y})\times\hat{\mathbf{x}}_2)\cdot(\bar{\mathbf{u}}^0\cdot\nabla\bar{\omega}^0 - \bar{\omega}^0\cdot\nabla\bar{\mathbf{u}}^0)dy\\ &\quad+\int_{\mathbb{T}^3} (\mathbf{k}^\varepsilon(\gamma^0(r_0)-\mathbf{y})\times\hat{\mathbf{x}}_2)\cdot(\mathbf{v}^0\cdot\nabla\bar{\omega}^0 - \bar{\omega}^0\cdot\nabla\mathbf{v}^0)dy\\ &\overset{(23)}{=} \int_{\mathbb{T}^3} (\mathbf{k}^\varepsilon(\gamma^0(r_0)-\mathbf{y})\times\hat{\mathbf{x}}_2)\cdot(\mathbf{v}^0\cdot\nabla\bar{\omega}^0 - \bar{\omega}^0\cdot\nabla\mathbf{v}^0)dy.\end{aligned}$$

We can neglect the second term (which takes into account the stretching effects) because

$$\begin{aligned}&\Big|\int_{\mathbb{T}^3} (\mathbf{k}^\varepsilon(\gamma^0(r_0)-\mathbf{y})\times\hat{\mathbf{x}}_2)\cdot(\bar{\omega}^0\cdot\nabla\mathbf{v}^0)dy\Big|\\ &\overset{(23)}{=} \Big|\int_{\mathbb{T}^3} (\mathbf{k}^\varepsilon(\gamma^0(r_0)-\mathbf{y})\times\hat{\mathbf{x}}_2)\cdot(\bar{\omega}_3^0\partial_3\mathbf{v}^0)dy\Big| \overset{(36)}{\lesssim} \frac{\Gamma\eta\|\bar{\omega}^0\|_\infty}{\varepsilon^2},\end{aligned}$$

where we also used that $\mathbf{k}^\varepsilon$ have uniformly bounded L^1 norm. Regarding the first term, using (23), it can be rewritten as

$$\partial_2\bar{\omega}_3^0(\gamma^0(r_0))\int_{\mathbb{T}^3} k_1^\varepsilon(\gamma^0(r_0)-\mathbf{y})v_2^0(\mathbf{y})dy + \int_{\mathbb{T}^3} k_1^\varepsilon(\gamma^0(r_0)-\mathbf{y})v_2^0(\mathbf{y})\big(\partial_2\bar{\omega}_3^0(\mathbf{y}) - \partial_2\bar{\omega}_3^0(\gamma^0(r_0))\big)dy.$$

The second term is an error, which satisfies the estimate

$$\Big|\int_{\mathbb{T}^3} k_1^\varepsilon(\gamma^0(r_0)-\mathbf{y})v_2^0(\mathbf{y})\big(\partial_2\bar{\omega}_3^0(\mathbf{y}) - \partial_2\bar{\omega}_3^0(\gamma^0(r_0))\big)dy\Big| \lesssim \Gamma\|\partial_2^2\bar{\omega}_3^0\|_\infty \tag{38}$$

proven below. The thesis will then follow from

$$\int_{\mathbb{T}^3} k_1^\varepsilon(\gamma^0(r_0)-\mathbf{y})v_2^0(\mathbf{y})dy \sim \frac{\Gamma}{4\pi}\ln\frac{1}{\varepsilon} \qquad \text{as } \varepsilon\to 0. \tag{39}$$

We have

$$\begin{aligned}\int_{\mathbb{T}^3} k_1^\varepsilon(\gamma^0(r)-\mathbf{y})v_2^0(\mathbf{y})dy &\overset{(21),(27)}{=} -\Gamma\int_{\mathbb{T}^3}\int_{\mathbb{T}} k_1^\varepsilon(\gamma^0(r_0)-\mathbf{y})k_1^\varepsilon(\mathbf{y}-\gamma^0(r))drdy\\ &= -\Gamma\int_{\mathbb{T}}(k_1^\varepsilon * k_1^\varepsilon)(\gamma^0(r_0)-\gamma^0(r))dr.\end{aligned} \tag{40}$$

Using Lemma 7, we learn that the main contribution to the last integral comes from the set $|r-r_0| \gg \varepsilon$. Indeed for $M = \ln^{\frac{1}{2}}(\varepsilon^{-1})$, we can split the last integral as

$$-\Gamma\int_{|r-r_0|\le M\varepsilon} k_1^\varepsilon * k_1^\varepsilon(\gamma^0(r_0)-\gamma^0(r))dr - \Gamma\int_{|r-r_0|>M\varepsilon} k_1^\varepsilon * k_1^\varepsilon(\gamma^0(r_0)-\gamma^0(r))dr.$$

From Lemma 7, we have $\|k_1^\varepsilon * k_1^\varepsilon\|_\infty \lesssim \varepsilon^{-1}$, which implies that the first term is $\Gamma \lesssim \ln^{\frac{1}{2}}(\varepsilon^{-1})$, hence is of lower order. Regarding the second term, it is equal to

$$\begin{aligned}&\frac{\Gamma}{4\pi}\int_{|r-r_0|>M\varepsilon}\frac{1}{|\gamma^0(r_0)-\gamma^0(r)|}\phi\Big(\frac{|\gamma^0(r_0)-\gamma^0(r)|}{\varepsilon}\Big)dr + O(\Gamma)\\ &= \Gamma\frac{1+o(1)}{4\pi}\int_{|r-r_0|>M\varepsilon}\frac{1}{|r-r_0|}dr + O(\Gamma) \qquad (\text{since}|\gamma^0(r_0)-\gamma^0(r)| \overset{\eta\ll 1}{\sim} |r-r_0| \gg \varepsilon)\\ &= \Gamma\frac{1+o(1)}{4\pi}\ln\frac{1}{M\varepsilon} + O(\Gamma) = \Gamma\frac{1+o(1)}{4\pi}\ln\frac{1}{\varepsilon} + O(\Gamma).\end{aligned}$$

This concludes the proof of (39). It remains to prove the error estimates (37) and (38).

Here comes the proof of (37). Starting from

$$\begin{aligned}v_2^t(\gamma^t(r_0)) &= -\Gamma\int_{\mathbb{T}}(\mathbf{k}^\varepsilon(\gamma^t(r_0)-\gamma^t(r))\times\hat{\mathbf{x}}_2)\cdot\partial_r\gamma^t(r)dr\\ &= -\Gamma\int_{\mathbb{T}} k_1^\varepsilon(\gamma^t(r_0)-\gamma^t(r))\partial_r\gamma_3^t(r)dr + \Gamma\int_{\mathbb{T}} k_3^\varepsilon(\gamma^t(r_0)-\gamma^t(r))\partial_r\gamma_1^t(r)dr\end{aligned}$$

and taking the derivative, we obtain

$$\begin{aligned}&\frac{d}{dt}v_2^t(\gamma^t(r_0))\Big|_{t=0}\\ &= -\Gamma\int_{\mathbb{T}}\nabla k_1^\varepsilon(\gamma^0(r_0)-\gamma^0(r))\cdot\big[\mathbf{v}^0(\gamma^0(r_0)) - \mathbf{v}^0(\gamma^0(r)) + \bar{\mathbf{u}}^0(\gamma^0(r_0)) - \bar{\mathbf{u}}^0(\gamma^0(r))\big]dr\\ &\quad-\Gamma\int_{\mathbb{T}} k_1^\varepsilon(\gamma^0(r_0)-\gamma^0(r))\partial_r\big(v_3^0(\gamma^0(r)) + \bar{u}_3^0(\gamma^0(r))\big)dr\\ &\quad+\Gamma\int_{\mathbb{T}} k_3^\varepsilon(\gamma^0(r_0)-\gamma^0(r))\partial_r\big(v_1^0(\gamma^0(r)) + \bar{u}_1^0(\gamma^0(r))\big)dr,\end{aligned} \tag{41}$$

where we used that $\partial_r\gamma_3^0(r) = 1$ and $\partial_r\gamma_1^0(r) = 0$ (see (21)).

Let us notice the following cancellation. Using that

$\partial_i k_j^\varepsilon(\mathbf{x}) = (|\mathbf{x}|^2+\varepsilon^2)^{-\frac{3}{2}}\delta_{ij} - 3x_ix_j(|\mathbf{x}|^2+\varepsilon^2)^{-\frac{5}{2}}$, together with $(\gamma^0(r_0)-\gamma^0(r))\cdot\hat{\mathbf{x}}_1 \overset{(21)}{=} 0$,

we obtain

$$\partial_2 k_1^\varepsilon(\gamma^0(r_0)-\gamma^0(r)) = \partial_3 k_3^\varepsilon(\gamma^0(r_0)-\gamma^0(r)) = 0. \tag{42}$$

Starting from (41), let us integrate by parts the last two terms. Using (42) and the fact that $\bar{u}_2^0 = \bar{u}_3^0 = 0$ (cf. (23)), one derives the following

$$\begin{aligned}\frac{d}{dt}v_2(t,\gamma^t(r_0))\Big|_{t=0} &= \Gamma\int_{\mathbb{T}}\partial_1 k_1^\varepsilon(\gamma^0(r_0)-\gamma^0(r))[v_1^0(\gamma^0(r_0)) - v_1^0(\gamma^0(r))]dr\\ &\quad+\Gamma\int_{\mathbb{T}}(\alpha'(r)\partial_2 k_3^\varepsilon + \partial_3 k_3^\varepsilon)(\gamma^0(r_0)-\gamma^0(r))v_1^0(\gamma^0(r))dr\\ &\quad+\Gamma\int_{\mathbb{T}}(\partial_1 k_1^\varepsilon + \alpha'(r)\partial_2 k_3^\varepsilon + \partial_3 k_3^\varepsilon)(\gamma^0(r_0)-\gamma^0(r))\big(\bar{u}_1^0(\gamma^0(r)) - \bar{u}_1^0(\gamma^0(r_0))\big)dr\\ &\quad+\bar{u}_1^0(\gamma^0(r_0))\Gamma\int_{\mathbb{T}}\big(\partial_3 k_3^\varepsilon(\gamma^0(r_0)-\gamma^0(r)) + \alpha'(r)\partial_2 k_3^\varepsilon(\gamma^0(r_0)-\gamma^0(r)\big)dr.\end{aligned}$$

Using (30) and (35), the first two terms are $\lesssim \Gamma^2\eta\varepsilon^{-3}$. From

$$\big|\bar{u}_1^0(\gamma^0(r_0)) - \bar{u}_1^0(\gamma^0(r))\big| \le \|(\bar{u}_1^0)'\|_\infty|\gamma_2^0(r_0)-\gamma_2^0(r)| \overset{(22)}{\le} \eta\|(\bar{u}_1^0)'\|_\infty|r-r_0| \overset{(24)}{=} \eta\|\bar{\omega}^0\|_\infty|r-r_0|$$

and (31) from Lemma 6, the third $\Gamma\eta\|\bar{\omega}^0\|_\infty\varepsilon^{-1}$. Finally, the last term is zero, since

$$\int_{\mathbb{T}}\big(\partial_3 k_i^\varepsilon(\gamma^0(r_0)-\gamma^0(r)) + \alpha'(r)\partial_2 k_i^\varepsilon(\gamma^0(r_0)-\gamma^0(r)\big)dr = -\int_{\mathbb{T}}\partial_r\big(k_i^\varepsilon(\gamma^0(r_0)-\gamma^0(r))\big)dr = 0.$$

To conclude, let us establish (38). We claim that

$$\int_{\mathbb{T}^3}\frac{1}{|\mathbf{x}-\mathbf{y}||\mathbf{y}|^2}dy \lesssim 1 + |\ln\frac{1}{|\mathbf{x}|}| \tag{43}$$

which follows from

$$\begin{aligned}\int_{\mathbb{T}^3}\frac{1}{|\mathbf{x}-\mathbf{y}||\mathbf{y}|^2}dy &\le \int_{B(0,1)}\frac{1}{|\mathbf{x}-\mathbf{y}||\mathbf{y}|^2}dy \overset{(\mathbf{y}=|\mathbf{x}|\mathbf{y}')}{=} \int_{B(0,\frac{1}{|\mathbf{x}|})}\frac{1}{|\frac{\mathbf{x}}{|\mathbf{x}|}-\mathbf{y}'||\mathbf{y}'|^2}dy'\\ &\lesssim 1 + \int_{B(0,\frac{1}{|\mathbf{x}|})\setminus B(0,2)}\frac{1}{|\mathbf{y}'|^3}dy' \lesssim 1 + \int_2^{\frac{1}{|\mathbf{x}|}}\frac{1}{\rho}d\rho \lesssim 1 + |\ln\frac{1}{|\mathbf{x}|}|.\end{aligned}$$

We then deduce (38)

$$\begin{aligned}&\Big|\int_{\mathbb{T}^3} k_1^\varepsilon(\gamma^0(r_0)-\mathbf{y})v_2^0(\mathbf{y})\big(\partial_2\bar{\omega}_3^0(\mathbf{y}) - \partial_2\bar{\omega}_3^0(\gamma^0(r_0))\big)dy\Big|\\ &\le \|\partial_2^2\bar{\omega}_3^0\|_\infty\int_{\mathbb{T}^3}|k_1^\varepsilon(\gamma^0(r_0)-\mathbf{y})||\gamma^0(r_0)-\mathbf{y}||v_2^0(\mathbf{y})|dy\\ &\overset{(27)}{\lesssim} \Gamma\|\partial_2^2\bar{\omega}_3^0\|_\infty\int_{\mathbb{T}}\int_{\mathbb{T}^3}\frac{1}{|\gamma^0(r_0)-\mathbf{y}||\gamma^0(r)-\mathbf{y}|^2}dydr\\ &= \Gamma\|\partial_2^2\bar{\omega}_3^0\|_\infty\int_{\mathbb{T}}\int_{\mathbb{T}^3}\frac{1}{|(\gamma^0(r_0)-\gamma^0(r))-\mathbf{y}||\mathbf{y}|^2}dydr\\ &\overset{(43)}{\lesssim} \Gamma\|\partial_2^2\bar{\omega}_3^0\|_\infty\int_{\mathbb{T}}\big(1+|\ln\frac{1}{|\gamma^0(r_0)-\gamma^0(r)|}|\big)dr \overset{(21)}{\lesssim} \Gamma\|\partial_2^2\bar{\omega}_3^0\|_\infty.\end{aligned}$$

□

4.2. The case of a thin domain

Consider the set

$$D = [0,1]\times[0,1]\times[0,\delta]$$

and call by $\mathbb{T}_\delta^3$ the set obtained from D by identification of the boundaries as in the case of a torus; all functions on $\mathbb{T}_\delta^3$ will be periodic, of period 1 in the two horizontal directions, period δ in the vertical direction.

In $\mathbb{T}^3_\delta$, consider a smooth curve of the form

$$\gamma(r) = \alpha(r)\hat{\mathbf{x}}_2 + r\hat{\mathbf{x}}_3$$

and a smooth background velocity field and the associated vorticity field, given by

$$\bar{\mathbf{u}}^0(\mathbf{x}) = \left(\bar{u}^0_1(x_2), 0, 0\right), \qquad \bar{\boldsymbol{\omega}}^0(\mathbf{x}) = \left(0, 0, \bar{\omega}^0_3(x_2)\right), \qquad \mathbf{x} \in \mathbb{T}^3_\delta.$$

Then introduce, on the classical torus $\mathbb{T}^3$, the curve

$$\tilde{\gamma}(s) = \tilde{\alpha}(s)\hat{\mathbf{x}}_2 + s\hat{\mathbf{x}}_3$$
$$\tilde{\alpha}(s) = \alpha(\delta s)$$

and the fields

$$\bar{\mathbf{u}}^{0,\delta}(\mathbf{x}) = \left(\bar{u}^0_1(x_2), 0, 0\right), \qquad \bar{\boldsymbol{\omega}}^{0,\delta}(\mathbf{x}) = \left(0, 0, \bar{\omega}^0_3(x_2)\right), \qquad \mathbf{x} \in \mathbb{T}^3.$$

If the original fields depended on x_3, the new ones would have been rescaled. But they were independent, hence we may drop the superscript δ from $\bar{\mathbf{u}}^{0,\delta}$ and $\bar{\boldsymbol{\omega}}^{0,\delta}$.

Given these initial conditions in the thin domain $\mathbb{T}^3_\delta$ and in the normalized domain $\mathbb{T}^3$, we may consider their time evolution. For the sake of the following result we call $\left(\gamma^t(r)\right)_r$ and $\left(\tilde{\gamma}^t(s)\right)_s$ the evolution at time t of the curves $(\gamma(r))_r$ and $(\tilde{\gamma}(s))_s$ respectively; using the equations of motion it is elementary to verify that $\partial_t^2 \tilde{\gamma}_2^{t=0}(s) = \partial_t^2 \gamma_2^{t=0}(\delta s)$.

If we set

$$\eta := \left\|\alpha'(r)\right\|_\infty$$

then

$$\left\|\tilde{\alpha}'(s)\right\|_\infty = \delta\eta.$$

Theorem 5 applies to $\tilde{\gamma}$, $\bar{\boldsymbol{\omega}}^0$ and gives us the following result. Assume $\partial_2\bar{\omega}^0_3\left(\tilde{\gamma}_2(s_0)\right) > 0$. In the limit $\varepsilon \ll 1$ and

$$\delta\eta \ll \varepsilon^3 \frac{\partial_2\bar{\omega}^0_3\left(\tilde{\gamma}_2(s_0)\right)}{\Gamma}$$

we have

$$\partial_t^2 \tilde{\gamma}_2^{t=0}(s_0) \sim \frac{\Gamma\partial_2\bar{\omega}^0_3\left(\tilde{\gamma}_2(s_0)\right)}{4\pi} \ln\frac{1}{\varepsilon}.$$

Call $r_0 = \delta s_0$. Then we have the following result in the thin domain $\mathbb{T}^3_\delta$:

Corollary 9. *If $\partial_2\bar{\omega}^0_3\left(\gamma_2(r_0)\right) > 0$, in the limit $\varepsilon \ll 1$ and*

$$\delta\eta \ll \varepsilon^3 \frac{\partial_2\bar{\omega}^0_3\left(\gamma_2(r_0)\right)}{\Gamma}$$

we have

$$\partial_t^2 \gamma_2^{t=0}(r_0) \sim \frac{\Gamma\partial_2\bar{\omega}^0_3\left(\gamma_2(r_0)\right)}{4\pi} \ln\frac{1}{\varepsilon}.$$

Remark 10. In the standard torus, we need (up to constants) $\eta \ll \varepsilon^3$, which looks quite severe, but we have to notice that we deal with a modification of a vertical straight line (namely a modification of the pure 2D case) which is global, affecting the whole length of the domain. In the case of a δ-thin domain, which is common in geophysical fluid dynamics and a very natural set-up for a quasi-2D theory, the condition becomes $\delta\eta \ll \varepsilon^3$ (up to constants), which is less severe.

5. Conclusions

With reference to the conceptual subdivision in the classes (a) and (b) of vortex structure interactions described in the Introduction, we focused on case (b), precisely on a concentrated 2D vortex structure of small radius in background shear flow, with a non-zero gradient of vorticity. We have proved a rigorous theorem about the motion along the gradient, confirming without any approximation a phenomenon previously identified on experimental and numerical basis, with certain approximate theoretical justifications. We have reached the explicit formula for the displacement in the orthogonal direction to the fluid flow

$$G_2(t) \sim \left(\frac{\Gamma\partial_2\bar{\omega}^0\left(\mathbf{x}^0\right)}{4\pi} \ln\frac{1}{\varepsilon}\right)t^2 \tag{44}$$

The first derivative is zero and the second derivative diverges as the radius ε of the vortex structure goes to zero (vortex point limit); numerically, this is confirmed by the log-log plots of the graph of $G_2(t)$, which in the limit as $\varepsilon \to 0$ behaves qualitatively as $G_2(t) \sim t^\alpha$ with powers α less than 2. A very vague fit gives $\alpha = \frac{3}{2}$ in an intermediate stage, before going down towards $\alpha = 1$ (or even less, but when time is so large that the peculiarities of the deformation of the background do not allow any more to deduce general principles). In spite of many attempts, we have not found an explanation of the power $\alpha = \frac{3}{2}$; therefore we are not sure if it is a true result or only the average indication of values smaller than 2, slowly changing around $\frac{3}{2}$.

Concerning the quasi-2D-flows, we have proved that a quasi-straight-line vortex filament in a shear flow performs a motion along the gradient, as in the 2D case. In order to handle such complex 3D system we have idealized a realistic vortex tube as a vortex filament (a curve) and we have paid the price of introducing a mollification of the Biot-Savart kernel at scale ε, the number that should describe the average radius of the tube. Three main open problems arose that we cannot treat in this work: a) generalize to a realistic vortex tube; b) find a threshold, like the one discussed in [33], beyond which the behaviour is different; c) identify special features, typical of the 3D case, even in the case under consideration where the motion along the gradient holds. In particular, about (c), from heuristic consideration we have the following conjecture.

i) where $\alpha''(r) < 0$, a larger concentration of background vorticity is created "behind" the vortex filament, which produces a stronger displacement, locally, of the filament along the gradient; with opposite behaviour where $\alpha''(r) > 0$;
ii) with the consequence of the beginning of an instability of the filament, eventually leading to an increase of deformation with respect to a vertical straight line.

However, the self-interaction of the vortex filament is so strong that perhaps the previous phenomena, even if existing, could be less relevant, and instabilities could occur more strongly for other reasons.

Among the perspective of our work there a rigorous analysis of stages of the dynamics which go beyond the first one, and analytical computations beyond the assumption of a small vorticity blob (clump or hole) in a background or larger vortex, approaching the case of vortices approximately of the same size. However it seems that these two problems require new techniques.

CRediT authorship contribution statement

Franco Flandoli: Writing – original draft, Validation, Supervision, Project administration, Methodology, Investigation, Conceptualization; **Matteo Palmieri:** Software, Methodology, Investigation, Formal analysis; **Milo Viviani:** Writing – original draft, Visualization, Software, Data curation.

Data availability

Data will be made available on request.

Declaration of competing interest

The authors declare the following financial interests/personal relationships which may be considered as potential competing interests:

Franco Flandoli reports financial support was provided by European Research Council. If there are other authors, they declare that they have no known competing financial interests or personal relationships that could have appeared to influence the work reported in this paper.

Acknowledgment

The research of F.F. is funded by the European Union, ERC NoisyFluid, No. 101053472 and the research project PRIN 2022 “Noise in fluid dynamics and related models”, no. 20222YRYSP. We thank the anonymous referees for an exceptionally deep list of remarks which was the basis for a massive reformulation of the manuscript and the addition of many results, in particular the quasi-two-dimensional case.

References

[1] Y. Zhou, Rayleigh–Taylor and Richtmyer–Meshkov instability induced flow, turbulence, and mixing. II, Phys. Rep. 723 (2017) 1–160.
[2] Y. Zhou, Hydrodynamic Instabilities and Turbulence: Rayleigh–Taylor, Richtmyer–Meshkov, and Kelvin–Helmholtz Mixing, Cambridge University Press, 2024.
[3] Y. Zhou, J.D. Sadler, O.A. Hurricane, Instabilities and mixing in inertial confinement fusion, Annu. Rev. Fluid Mech. 57 (2025) 197–225.
[4] G. Boffetta, R.E. Ecke, Two-dimensional turbulence, Annu. Rev. Fluid Mech. 44 (1) (2012) 427–451.
[5] P.B. Rhines, Waves and turbulence on a beta-plane, J. Fluid Mech. 69 (3) (1975) 417–443.
[6] A.R. Vasavada, A.P. Showman, Jovian atmospheric dynamics: an update after galileo and cassini, Rep. Prog. Phys. 68 (8) (2005) 1935.
[7] P.H. Diamond, S.I. Itoh, K. Itoh, T.S. Hahm, Zonal flows in plasma–a review, Plasma Phys. Control. Fusion 47 (5) (2005) R35.
[8] A. Hasegawa, K. Mima, Stationary spectrum of strong turbulence in magnetized nonuniform plasma, Phys. Rev. Lett. 39 (4) (1977) 205.
[9] G.K. Vallis, Atmospheric and Oceanic Fluid Dynamics, Cambridge University Press, 2017.
[10] R.J. Briggs, J.D. Daugherty, R.H. Levy, Role of Landau damping in crossed-field electron beams and inviscid shear flow, Phys. Fluids 13 (2) (1970) 421–432.
[11] W. Horton, A. Hasegawa, Quasi-two-dimensional dynamics of plasmas and fluids, Chaos Interdiscip. J. Nonlinear Sci. 4 (2) (1994) 227–251.
[12] E. Özuğurlu, J.N. Reinaud, D.G. Dritschel, Interaction between two quasi-geostrophic vortices of unequal potential vorticity, J. Fluid Mech. 597 (2008) 395–414.
[13] F.H. Krajchnan, Inertial ranges in two-dimensional turbulence, Phys. Fluids 10 (1967) 1417.
[14] J. Von Hardenberg, J.C. McWilliams, A. Provenzale, A. Shchepetkin, J.B. Weiss, Vortex merging in Quasi-geostrophic flows, J. Fluid Mech. 412 (2000) 331–353.
[15] A.H. Nielsen, X. He, J.J. Rasmussen, T. Bohr, Vortex merging and spectral cascade in two-dimensional flows, Phys. Fluids 8 (9) (1996) 2263–2265.
[16] J.N. Reinaud, D.G. Dritschel, The merger of vertically offset quasi-geostrophic vortices, J. Fluid Mech. 469 (2002) 287–315.
[17] A. Sánchez-Lavega, J.F. Rojas, R. Hueso, J. Lecacheux, F. Colas, J.R. Acarreta, I. Miyazaki, D. Parker, Interaction of jovian white ovals BC and DE in 1998 from earth-based observations in the visual range, Icarus 142 (1) (1999) 116–124.
[18] P.S. Marcus, T. Kundu, C. Lee, Vortex dynamics and zonal flows, Phys. Plasmas 7 (5) (2000) 1630–1640.
[19] P.S. Marcus, Prediction of a global climate change on Jupiter, Nature 428 (6985) (2004) 828–831.
[20] M.H. Wong, I. de Pater, X. Asay-Davis, P.S. Marcus, C.Y. Go, Vertical structure of Jupiter’s oval BA before and after it reddened: what changed?, Icarus 215 (1) (2011) 211–225.
[21] A. Ogawa, A. Sanpei, H. Himura, Convective vortex merging in electron plasma, Phys. Plasmas 32 (6) (2025).
[22] C. Marchioro, M. Pulvirenti, On the vortex–wave system, in: Mechanics, Analysis and Geometry: 200 Years after Lagrange, Elsevier, 1991, pp. 79–95.
[23] T.H. Dupree, Growth of phase-space density holes, Phys. Fluids 26 (9) (1983) 2460–2481.
[24] G.F. Carnevale, R.C. Kloosterziel, G.J.F. Van Heijst, Propagation of barotropic vortices over topography in a rotating tank, J. Fluid Mech. 233 (1991) 119–139.
[25] J.C.L. Chan, R.T. Williams, Analytical and numerical studies of the beta-effect in tropical cyclone motion. part i: zero mean flow, J. Atmos. Sci. 44 (9) (1987) 1257–1265.
[26] X. Li, B. Wang, Barotropic dynamics of the beta gyres and beta drift, J. Atmos. Sci. 51 (5) (1994) 746–756.
[27] X. Garbet, Y. Idomura, L. Villard, T.H. Watanabe, Gyrokinetic simulations of turbulent transport, Nucl. Fusion 50 (4) (2010) 043002.
[28] D.G. Dritschel, A general theory for two-dimensional vortex interactions, J. Fluid Mech. 293 (1995) 269–303.
[29] F. Flandoli, Renormalized onsager functions and merging of vortex clusters, Stoch. Dyn. 20 (06) (2020) 2040010.
[30] M. Amoretti, D. Durkin, J. Fajans, R. Pozzoli, M. Romé, Asymmetric vortex merger: experiments and simulations, Phys. Plasmas 8 (9) (2001) 3865–3868.
[31] I.M. Lansky, T.M. O’Neil, D.A. Schecter, A theory of vortex merger, Phys. Rev. Lett. 79 (8) (1997) 1479.
[32] D.A. Schecter, D.H.E. Dubin, Vortex motion driven by a background vorticity gradient, Phys. Rev. Lett. 83 (11) (1999) 2191.
[33] A. Alexakis, Quasi-two-dimensional turbulence, Rev. Mod. Plasma Phys. 7 (1) (2023) 31.
[34] A. Mariotti, B. Legras, D.G. Dritschel, Vortex stripping and the erosion of coherent structures in two-dimensional flows, Phys. Fluids 6 (12) (1994) 3954–3962.
[35] L.S. Da Rios, On the motion of an unbounded fluid with a vortex filament of any shape, Rend 22 (1906) 117.
[36] T. Levi-Civita, Teoremi di unicita e di esistenza per le piccole oscillazioni di un filetto vorticoso prossimo alla forma circolare (uniqueness and existence theorems for small oscillations of a vortex filament near the circular shape, Rend. R. Acc. Lincei 15 (1932) 409–416.
[37] P.G. Saffman, Vortex dynamics, in: Theoretical Approaches to Turbulence, Springer, 1992, pp. 263–277.
[38] J.P. Keener, Knotted vortex filaments in an ideal fluid, J. Fluid Mech. 211 (1990) 629–651.
[39] R.L. Ricca, Rediscovery of da Rios equations, Nature 352 (6336) (1991) 561–562.
[40] Y. Fukumoto, T. Miyazaki, Three-dimensional distortions of a vortex filament with axial velocity, J. Fluid Mech. 222 (1991) 369–416.
[41] A.J. Majda, A.L. Bertozzi, Vorticity and Incompressible Flow, Cambridge Texts in Applied Mathematics, Cambridge University Press, 2001.
[42] D. Benedetto, E. Caglioti, C. Marchioro, On the motion of a vortex ring with a sharply concentrated vorticity, Math. Methods Appl. Sci. 23 (2) (2000) 147–168.
[43] F. De la Hoz, L. Vega, Vortex filament equation for a regular polygon, (2013). arXiv:1304.5521.
[44] R.L. Jerrard, C. Seis, On the vortex filament conjecture for Euler flows, Arch. Ration. Mech. Anal. 224 (1) (2017) 135–172.
[45] V. Banica, L. Vega, Evolution of polygonal lines by the binormal flow, Ann. PDE 6 (1) (2020) 6.
[46] V. Banica, D. Eceizabarrena, A.R. Nahmod, L. Vega, Multifractality and intermittency in the limit evolution of polygonal vortex filaments, Math. Ann. 391 (2) (2025) 2837–2899.
[47] M.A. Fontelos, L. Vega, Evolution of viscous vortex filaments and desingularization of the Biot-Savart integral, (2023). arXiv:2311.12246.
[48] P. Buttà, C. Marchioro, Long time evolution of concentrated Euler flows with planar symmetry, SIAM J. Math. Anal. 50 (1) (2018) 735–760.
[49] C. Marchioro, M. Pulvirenti, Mathematical Theory of Incompressible Nonviscous Fluids, 96, Springer Science & Business Media, 2012.
[50] E. Caglioti, P.-L. Lions, C. Marchioro, M. Pulvirenti, A special class of stationary flows for two-dimensional Euler equations: a statistical mechanics description. part II, Commun. Math. Phys. 174 (1995) 229–260.
[51] P.-H. Chavanis, Statistical mechanics of two-dimensional point vortices: relaxation equations and strong mixing limit, Eur. Phys. J. B 87 (2014) 1–24.
[52] G.L. Eyink, H. Spohn, Negative-temperature states and large-scale, long-lived vortices in two-dimensional turbulence, J. Stat. Phys. 70 (1993) 833–886.
[53] G.L. Eyink, K.R. Sreenivasan, Onsager and the theory of hydrodynamic turbulence, Rev. Mod. Phys. 78 (1) (2006) 87–135.
[54] P.-L. Lions, On Euler Equations and Statistical Physics, Scuola Normale Superiore (Edizioni della Normale, 1997).
[55] D. Montgomery, G. Joyce, Statistical mechanics of negative temperature states (1973).
[56] L. Onsager, Statistical hydrodynamics, Il Nuovo Cimento (1943-1954) 6 (Suppl 2) (1949) 279–287.
[57] D.W. Moore, P.G. Saffman, Structure of a line vortex in an imposed strain (1971) 339–354.
[58] V.I. Yudovich, Non-stationary flow of an ideal incompressible liquid, USSR Comput. Math. Math. Phys. 3 (6) (1963) 1407–1456.
[59] V. Bogomolov, Dynamics of vorticity at a sphere, Fluid Dyn. 6 (1977) 863–870.
[60] F. Laurent-Polz, Point vortices on a rotating sphere, Regul. Chaotic Dyn. 10 (1) (2005) 39–58.
[61] V. Zeitlin, Self-consistent finite-mode approximations for the hydrodynamics of an incompressible fluid on nonrotating and rotating spheres, Phys. Rev. Lett. 93 (26) (2004) 264–501. https://doi.org/10.1103/PhysRevLett.93.264501
[62] K. Modin, M. Viviani, A brief introduction to matrix hydrodynamics, (2025). arXiv:2508.07088.
[63] K. Modin, M. Viviani, A Casimir preserving scheme for long-time simulation of spherical ideal hydrodynamics, J. Fluid Mech. 884 (22A) (2020). https://doi.org/10.1017/jfm.2019.944
[64] D. Cordoba, C. Fefferman, On the collapse of tubes carried by 3D incompressible flows, (2001). arXiv:math/0101253.
[65] H. Bessaih, M. Coghi, F. Flandoli, Mean field limit of interacting filaments and vector valued non-linear PDEs, J. Stat. Phys. 166 (5) (2017) 1276–1309.
[66] L.C. Berselli, H. Bessaih, Some results for the line vortex equation, Nonlinearity 15 (6) (2002) 1729.